UNIVERSIDADE DE LISBOA

FACULDADE DE CIÊNCIAS

DEPARTAMENTO DE FÍSICA

Development of an upper limb exoskeleton digital twin in immersive virtual reality

Tiago Manuel Cortes Lomba

Mestrado em Engenharia Biomédica e Biofísica

Dissertação orientada por:

Dr. Nuno Miguel de Pinto Lobo e Matela

Dr. Laura Marchal-Crespo

2023

‘Whatever the mind can conceive and believe, the mind can achieve.”

-Napoleon Hill

Acknowledgments

First of all, I would like to express my deepest gratitude to gratitude to all those who provided me the opportunity to carry out this internship. I want to thank my thesis supervisor Dr. Laura Marchal-Crespo, who gave me the opportunity to complete this internship and work in an exceptional team. I would also like to thank her for believing in my abilities and challenging me to improve. Thank you for everything, I was very lucky.

To my internal supervisor Alex Ratschat, I really want to thank you for all the patience, continuous guidance, and smart and clear way of explaining science. I am grateful for all the advice and knowledge that I have received.

I would also like to thank Professor Nuno Matela, from the Faculty of Science of the University of Lisbon, for all the support this year and his great willingness to help me whenever I needed it.

To all MSc and Ph.D. students in the Cognitive Robotics department, I want to express my appreciation for helping me when I needed it and for always making me feel welcome. A special thanks to Joseph who quickly became a great companion and friend, for making the work feel easier and this experience more enjoyable (and for the great coffee breaks).

I also want to thank all the staff at the VR Zone in TU Delft for helping me rapidly develop skills in virtual reality development. A special thanks to Sharif for his willingness and patience to help me whenever I needed it.

I want to thank my family for always supporting and believing in me. I would like to thank my parents for all the opportunities and guidance they have given me, which have made it possible for me to get this far. I want to thank them for making this opportunity possible and for always caring about me. To my sister, thank you for sticking with me throughout this journey.

I want to express my gratitude to all my friends who accompanied me on this journey and helped me in different ways. Without them, this journey would have been much more difficult and boring. Thank you for coming into my life and staying in it for all these years.

Finally, I want to thank Patricia for always being with me throughout this journey and for being my safe haven. For all the lunch boxes and dinners, she lovingly prepared for me, for helping me when I was stressed, for her dedication to saving money, for helping me to be a better person, and for all the good times we had during this experience. Once again, thank you.

Abstract

Research suggests that for stroke patients, high-intensity training is critical for patient recovery. This can be provided by robotic rehabilitation in combination with virtual reality (VR), enabling highly intensive and motivating exercises.

The more motivated the patients are, the more engaged they will be in performing the exercises, ultimately leading to better motor function improvement. However, in conventional therapy and most research, the robot is usually not visualized, which can lead to a discrepancy between what the user sees and feels.

In this work, we present the development of a digital twin of an upper limb rehabilitation exoskeleton in VR. The user interacted with the virtual environment (VE) through a head-mounted display and manipulation of the real robot. To create a more functional and realistic interaction with the VE, the exoskeleton was previously upgraded with one more degree of freedom, by integrating a novel hand module, allowing the user to perform grasping movements. In addition, a prototype of a VR game aimed at the interaction between the digital twin and the VE was developed, as well as preliminary measurements of the kinematic accuracy of the digital twin and its kinematic model.

When the user moved the rehabilitation robot, the digital twin was found to move accordingly, mimicking the movements of all joints. With only a small position offset, it can be concluded that despite the exoskeleton's complexity, the implementation was successful, and this offset will probably not reduce the immersion or embodiment of the user.

The developed visualization enables the possibility of studying the influence of digital twins on motor learning. Although future work is needed, namely adjusting the joints of the digital twin, and testing the visualization model on real patients, this study should be considered as a starting point to allow the development of more effective rehabilitation exercises.

Keywords: stroke, upper limb, robotic rehabilitation, virtual reality, digital twin

Resumo

O AVC é uma condição em que o fluxo sanguíneo que transporta oxigénio e nutrientes para o cérebro é interrompido. É uma das principais causas de morte e incapacidade em todo o mundo, com até 75% dos sobreviventes a acabarem com deficiências dos membros superiores. Um controlo motor insuficiente compromete a capacidade dos doentes com AVC de realizar atividades da vida quotidiana (do inglês ADLs) e terá provavelmente um impacto negativo na qualidade de vida. Embora a recuperação da função motora ser essencial, mais de 50% têm um défice contínuo dos membros superiores.

Os processos de reabilitação devem envolver uma formação ativa e intensa, durante um longo período, e com alguns componentes desafiantes para maximizar a recuperação. Além disso, os primeiros três meses após um AVC são o tempo em que ocorre a maior parte da recuperação motora. Neste sentido, é importante maximizar a reabilitação durante este período.

A terapia assistida por robot consegue proporcionar treinos de alta intensidade, reduzir a sobrecarga os terapeutas e medir objetivamente as funções biomecânicas dos membros como a amplitude de movimento e, portanto, o desempenho e progresso do paciente. No entanto, esta é repetitiva e o processo de reabilitação pode tornar-se monótono, o que acaba por afetar a recuperação do doente devido à falta de motivação.
Com o acréscimo de realidade virtual, é possível implementar exercícios que motivem o paciente, podendo adaptar-se o exercício às características do mesmo. Enquanto o ambiente virtual (VE, do inglês virtual environment) é normalmente apresentado num ecrã 2D, a utilização do ecrã montado na cabeça (HMD, do inglês Head-mounted display) permite dar ao utilizador uma maior sensação de estar no cenário virtual, conceito conhecido como realidade virtual imersiva (IVR, do inglês immersive virtual reality). Quanto mais imersiva for a realidade virtual, mais o utilizador se sentirá presente, o que o tornará mais propenso a interagir com os estímulos e o VE.

Contudo, na maioria dos sistemas IVR atualmente em uso, os utilizadores interagem com o VE utilizando principalmente controladores em vez de dispositivos robóticos de assistência. Além disso, o robô de assistência raramente é visualizado no VE, criando um desajuste entre o que o utilizador sente e vê. Assim, é notória a falta de provas sobre como a interação com o VE enquanto se utiliza um robô e a sua visualização pode influenciar a recuperação motora e a motivação, bem como a forma como pode ser utilizado para alterar ou melhorar as tarefas de reabilitação.

Esta dissertação possuí dois objetivos principais. Primeiro, a integração de módulo manual pré-existente no robô exosqueleto para reabilitação dos membros superiores com seis graus de liberdade ARMin. Esta integração tem como intuito permitir a realização de exercícios de reabilitação mais complexos em linha com as atividades da vida quotidiana (ADLs), aumentando ao mesmo tempo os graus de liberdade do robô. O segundo objetivo desenvolver um gémeo digital (do inglês digital twin, DT) deste mesmo robô num VE, com o objetivo de permitir ao paciente não só ver exatamente os movimentos que estava a fazer, em realidade virtual, mas também o robô em que se encontrava, retratando com precisão a realidade em que se encontrava.

A metodologia para este estudo consistiu no design e fabricação, através do programa de modelação Fusion 360 e de impressão 3D, de quatro peças que permitiram que o módulo da mão denominado PRIDE fosse integrado no exosqueleto ARMin, substituindo o sector final (do inglês End-Effector, EE) que este possuía anteriormente. O módulo manual PRIDE, desenvolvido por *Rätz et al.* [1] é capaz de oferecer, com uma configuração sem esforço,

uma gama de movimento de 180º para flexão e extensão dos dedos, enquanto dá uma confortável aderência ao utilizador. As pegas de tamanho específico (pequenas, pequenas-médias, médias-grandes, grandes) podem ser colocadas e trocadas, para que se ajustem ao tamanho da mão do utilizador.
Posteriormente, o modelo 3D do robô exosqueleto foi dividido em cada uma das suas juntas, sendo configurado o eixo de rotação/translação de cada no programa Blender e posteriormente importada para o programa Unity, onde foram desenvolvidos o VE e o DT deste exosqueleto. Assim, foram conectadas e configuradas todas as juntas, de modo a movimentar-se de forma semelhante à realidade. Foi ainda implementado o dispositivo do módulo da mão, anteriormente colocado no exosqueleto, no VE. Por fim, foi adicionado um modelo de uma mão humana, sendo o movimento desta e do PRIDE animado durante todo o movimento de 180º.

Para recuperar os dados do modelo cinemático do ARMin, relativamente aos ângulos das articulações e respetivas coordenadas, em tempo real no VE, foram desenvolvidos vários scripts utilizando a linguagem de programação C# e o protocolo de comunicação *User Datagram Protocol* (UDP). Para imitar o movimento real, foi primeiro necessário posicionar cada junta rotacional no VE na posição marcada no modelo cinemático como 0°. A partir desta posição inicial, foi desenvolvido um código que gradualmente ajustava a posição de cada junta com base na diferença para o estado anterior. Para as juntas que se deslocaram horizontalmente, foi registado quais eram os limites máximos de cada uma, ou seja, qual o valor máximo que a articulação podia tomar quando movida totalmente para trás e quando movida para a frente. Estes valores foram medidos utilizando o modelo cinemático do robô, obtendo-se o intervalo. Depois, a mesma lógica foi aplicada ao VE, onde a junta foi movida para cada um dos seus limites e registou-se o valor de posição no Unity em cada caso. Finalmente, e utilizando a função *remap* do pacote de *Mathematics* em C#, foi possível remapear linearmente o valor de posição x de cada junta de modo a cada valor do modelo cinemático do robô corresponde-se a um valor no VE.

Para incorporar a realidade virtual no ambiente virtual já desenvolvido, foi necessário um HMD. O HMD escolhido foi o *Varjo-XR*. Ainda foi necessário a utilização de duas estações base HTC e de um localizador *HTC VIVE*, para registar a posição e movimento do HMD e para colocar o DT na mesma posição que o robô real. Para testar o VE, foi ainda desenvolvido um jogo em realidade virtual. Este consistia na construção da pirâmide de seis cubos. Para isso, o utilizador teria de agarrar cada cubo, através da movimentação do robô, e colocá-lo num dos alvos sobre a mesa. Quando completada a tarefa, o utilizador era deparado com quanto tempo demorou a realizá-la. De modo a testar também a exatidão do modelo cinemático do exosqueleto e a exatidão do seu DT, foram realizadas algumas medições preliminares: medição da posição do *end-effector* em cinco pontos e em duas alturas da mesa, e medição dessa mesma posição aquando da realização de várias poses que hipoteticamente poderiam ser realizadas durante exercícios de reabilitação.

Os nossos resultados sugerem que a integração do módulo de mão permitiu ao utilizador realizar movimentos de agarrar. Sendo este um dos movimentos essenciais praticados nos ADLs, permitirá ao utilizador realizar exercícios de reabilitação mais completos. Relativamente ao DT, cada articulação foi implementada e conectada de modo a gerar um sistema cinemático semelhante ao do robô real. O DT foi ligado ao exoesqueleto, recuperando os seus dados, e imitando os seus movimentos. A utilização de VR em vez de um ecrã de computador para visualizar e interagir com o DT criou condições para desenvolver exercícios de reabilitação mais imersivos e motivadores. Através da avaliação da precisão cinemática, verificou-se que o desvio de posição entre o robô real e o DT era baixo e, portanto, sugere que para valores baixos na gama de centímetros, o utilizador não será afectado em termos de imersão. Além disso, conseguimos realizar tarefas simples no VE com o DT, permitindo-lhe interagir com o VE e criar exercícios de reabilitação relevantes com base nisso.

Os próximos passos no desenvolvimento deste dispositivo serão uma melhor configuração das articulações e do VE e a implementação da comunicação do módulo da mão com o VE, uma vez que devido a restrições de tempo, não o foi possível efetuar. Relativamente ao dispositivo de módulo manual, são também necessários alguns ajustes, nomeadamente em relação ao material que constitui as peças, que devem ser mais robustas e resistentes. Finalmente, o trabalho futuro deve envolver sujeitos a testar o DT desenvolvido e o VE, a fim de receber feedback sobre fatores como a imersão e a dificuldade de realizar as tarefas, incluindo possivelmente pacientes reais que apresentam dificuldades motoras resultantes de um AVC.

Este estudo abre possibilidades de investigação inovadoras. Em primeiro lugar, uma vez que o DT e o VE são totalmente personalizáveis, permite-nos estudar como o utilizador reage às diferentes características e como isto influência a recuperação do motor. Principalmente, podemos avaliar que características influenciam positivamente a recuperação motora do utilizador e criar exercícios mais personalizados. Além disso, esperamos que o nosso trabalho aumente a sensibilização para a aplicabilidade do DT no campo da reabilitação. O nosso estudo poderá então contribuir para o estudo e compreensão de melhores processos de reabilitação após o AVC, melhorando a recuperação pós AVC das pessoas e melhorando assim a sua qualidade de vida futura.

Palavras-chave: AVC, membro superior, reabilitação robótica, realidade virtual, gémeo digital

Contents

List of Figures

List of Tables

List of Abbreviations

2D – Two-Dimensions

3D – Three-Dimensions

ADLs – Activities of Daily Living

AR – Augmented Reality

BDNF – Brain Derived Neurotrophic Factor

CIMT – Constrain-Induced Movement Therapy

CT – Computerized Tomography

DoF – Degrees of Freedom

DT – Digital Twin

EE – End-Effector

FK – Forward Kinematics

FMA – Fugl-Meyer Assessment

HDRP - High-Definition Render Pipeline

HMD – Head-Mounted Display

IVR – Immersive Virtual Reality

MCP - Metacarpophalangeal

MR – Mixed Reality

MRI – Magnetic Resonance Imaging

MSS – Motor Status Score

MT – Mirror Therapy

PLA - Polylactic acid

RR – Real Robot

TrkB - Tropomyosin-Receptor Kinase B

UDP – User Datagram Protocol

UL – Upper Limb

VE – Virtual Environment

VR – Virtual Reality

WMFT – Wolf Motor Function Test

XR – Extended Reality

1. Introduction

Stroke remains one of the leading causes of death and disability worldwide [2], with up to 75% of survivors ending up with upper limb disabilities [3]. These affect their activities of daily living (ADLs) by limiting their grasping and reaching movements and, ultimately, their quality of life. Although recovering upper extremity motor function is essential for stroke patients to take care of themselves and perform ADLs [4], only 35-70% of stroke survivors regain functional levels of arm mobility and more than 50% have ongoing upper extremity deficits [5].

Rehabilitation processes should involve active and intense training over a long period of time and with some challenging components to it to maximize recovery [6]. Furthermore, the first three months after a stroke is the time when most motor recovery occurs [7]. In this sense, it is essential to maximize rehabilitation during this period. Robotic therapy can provide high-intensity and repetition-focused training while reducing the burden on therapists [8]. Compared to conventional therapy, the number of repetitions that can be achieved is much higher, reaching more than 1000 movements compared to 45 of conventional stroke therapy [9]. However, the repetition of tasks during robotic therapy can become monotonous, ultimately affecting the patient's recovery due to a lack of motivation [10]. For that reason, the patient must be engaged and motivated while performing the task. These two specific aspects have been described as crucial for improving neurorehabilitation [11].

By combining robotic rehabilitation with virtual reality (VR), it is possible to implement engaging and motivational exercises. These can not only provide meaningful task-oriented exercises but adapt parameters such as feedback (e.g., haptic or auditory), duration, and intensity, to the needs of the individual patient, demonstrating improvements in upper extremity functions [12]–[14]. An essential factor for an effective virtual environment is the consensus between proprioceptive information and sensory feedback [15]. While VR can also be on a 2D screen, the use of a head-mounted display (HMD) allows it to give the user a greater sense of being in the virtual setting [12]. If that is the case, we refer to it as an immersive virtual reality (IVR). The main goal of immersive VR is to give the user a sense of presence, the illusion of being in the rendered place, which makes them more likely to interact with the stimuli and the virtual environment. The more accurately the body motions are recreated and matched, the more immersive the environment is [16], [17].

However, in most of the IVR systems currently in use, users interact with the virtual environment (VE) primarily using controllers rather than assistive robotic devices. [18]–[21]. Further, the assistive robot is rarely visualized in the VE, creating a mismatch between what the user feels and sees. Hence, it is noteworthy that there is a lack of evidence on how the interaction with the VE while using a robot and its visualization can influence motor recovery and motivation, as well as how it can be used to alter or improve rehabilitation tasks.

To this end, a digital twin of the ARMin upper limb rehabilitation exoskeleton was developed in a virtual environment, allowing the user to see the arm and robot movements in VR, accurately portraying the user's reality. The term "digital twin" has become of increasing interest among researchers. However, few studies have yet been done on their applications, especially in rehabilitation. Thus, in this study, we present the development of a digital twin of a complex rehabilitation robot used for upper limb rehabilitation. To allow for better interaction with the VE and more complex rehabilitation exercises in line with ADLs, a hand module was first integrated into the exoskeleton. Furthermore, to enable a preliminary evaluation of the digital twin and its behaviour, an assessment of the accuracy of the kinematic model of the exoskeleton and its digital twin was performed and a prototype of a virtual reality game was developed.

This manuscript is divided into six chapters. The theoretical background required to comprehend this work is presented in chapter 2. In chapter 3, it is explained how the hand module was integrated and how the creation and visualization of an upper limb rehabilitation exoskeleton’s digital twin were made. Chapter 4 presents the study's findings, and chapter 5 discusses them. General conclusions are provided in chapter 6.

2. Background

2.1. Stroke

Stroke is a condition where the blood flow that carries oxygen and nutrients to the brain is interrupted. This can happen through a clot obstructing the brain's blood supply, an ischemic stroke (approximately 80% of the cases), or through a rupture of a blood vessel, a hemorrhagic stroke (approximately 20% of the cases) [22]. These conditions create an environment of hypoxia and glucose deprivation that leads to neuronal death [23].
Ischemic strokes can be categorized based on etiology. The most common subtype is atherosclerosis, i.e., thickening or hardening of the arteries caused by the buildup of plaque (fatty deposits) in the inner lining of the great arteries [24]. It is characterized by infarcts, i.e., larger than 15 to 20 mm, involving the cortex, cerebellum, brainstem, and subcortical regions. The most typical cause is by large vessel disease brought on by atherosclerosis of the cervical or proximal intracranial vessels, which is a significant cause of acute infarcts (30%-43%) [25] Other categories are: cardioembolic sources, i.e, sources that cause a blockage inside a blood vessel, responsible for 20%–31% of acute ischemic infarcts; small artery occlusions, which are likely to be responsible for infarcts smaller than 20 mm and account for 10%–23% of acute infarcts; or abnormal causes (2%–11%), such as vasculopathy, i.e., vascular lesion, involving proximal vessels, which may cause territorial infarcts of perforating vessels supplying deep white matter and the basal ganglia [26]. Hemorrhagic strokes, on the other hand, are mainly caused by hypertension. Hypertensive strokes occur at typical sites, including the basal ganglia, thalamus, pons, and cerebellum [27].

Brain scanning techniques such as magnetic resonance imaging (MRI), or computerized tomography (CT) have a critical role in early stroke diagnosis. In addition to aiding in the diagnosis of acute stroke, patterns of infarction on imaging can help distinguish irreversible infarcted tissues from salvageable tissue and suggest a possible cause, which not only influences the immediate treatment planning but also identifies appropriate secondary prevention therapies to prevent stroke recurrence. An illustrative example of an MRI and CT scan is presented in Figure 2.1.

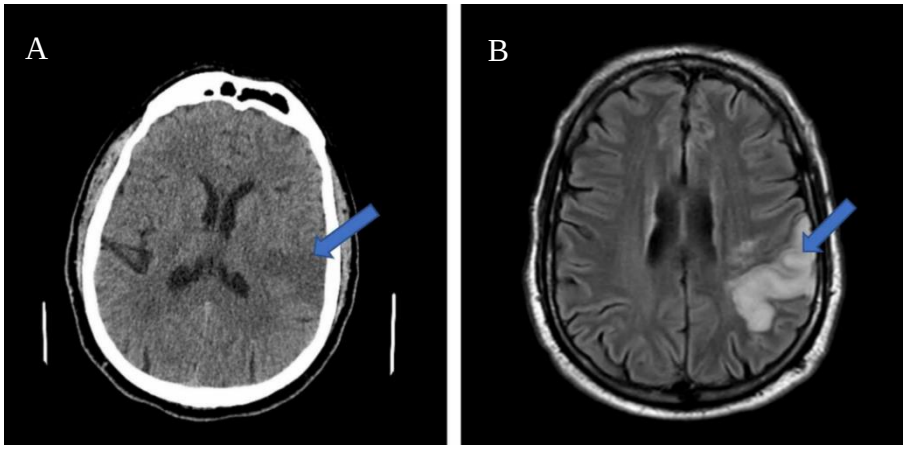

Figure 2.1 *- (A) CT scan of the head and (B) MRI of the brain showing an evolving moderate-sized subacute left MCA branch infarct (arrows). Figure adapted from* [28].

Major risk factors for stroke include hypertension, hyperlipidemia, diabetes mellitus, and smoking. However, a substantial portion of strokes can be prevented if these risk factors are monitored.
It remains the most acquired neurological disease in the adult population, mainly affecting patients over 65. Only 1 in 5 survivors lives more than ten years [29], while only 1 in 10 survive for 20 years [30]. The most critical factors for long-term stroke survival are age at the time of the event, followed by the severity of the stroke, functional level, and cardiovascular risk factors. However, life expectancy after a stroke has been increasing gradually thanks to factors such as the improvement in care and prevention and the increased life expectancy in the general population [31].

A stroke significantly alters the complexity of neural networks within the affected area, which is projected toward cognitive and motor function impairments and leads to a loss of functional performance capacity [32]. People after a stroke may experience different degrees of impairment (mid, acute, and severe) in different hemispheres (left, right, or both), as well as different levels: upper (face, neck), medium (trunk, upper limbs), and lower (lower limbs).

One of the most common and recognized after-stroke effects is hemiparesis, which is muscular weakness or partial paralysis on one side of the body. It is registered in 88% of people after stroke, impacting the lower but, most commonly, upper limbs [33]. In fact, up to 75% of stroke survivors end up with upper limb impairment [3]. Other common impairments include speech and language difficulties, swallowing, vision defect, and impaired cognition [34].

Many activities of daily living (ADLs) involve the upper limbs, e.g., eating, writing, and personal hygiene. These tasks demand complicated movement patterns that link the activation of the necessary muscle groups with the sensorimotor coordination of the hands to produce an efficient functional action. However, post-stroke upper limb impairment results in muscle weakness, as well as a decrease in movement precision and coordination. Therefore, people after a stroke with upper limb impairment have limited grasping and reaching movement capabilities, ultimately affecting their quality of life. Consequently, regaining the lost function in the upper limbs is crucial for the patient.

2.2. Conventional Rehabilitation

Although substantial improvements have been made in treating acute stroke, rehabilitation still makes up most of the care provided to reduce the long-term effects and achieve optimal functional recovery for patients [35]. Stroke rehabilitation focuses primarily on recovering impaired movement to reduce disability and promote participation in everyday activities. It is crucial to minimize the long-term effects of stroke and obtain the best functional recovery for reintegration into the community.

Reacquiring this motor function is possible through neuroplasticity, the intrinsic ability of the brain to rearrange and form new connections in response to stimuli and injuries [36]–[38].
The effectiveness of neuroplasticity relies on a molecule that promotes the growth and survival of neurons called brain-derived neurotrophic factor (BDNF) [39]. By attaching to tropomyosin-receptor kinase B (TrkB), BDNF plays a significant role in neuron development, synaptic transmission, and neurotransmitter production [40]. Yet, to trigger neuroplasticity's growth, the brain cells need to be stimulated by exposing them to regular activities in a person's daily life. Consequently, to promote neuroplasticity and achieve an

optimal outcome for the individual patient, rehabilitation processes should involve active and intense training over a long period, with some challenging components to maximize recovery.
Furthermore, most motor recovery occurs in the first three months after a stroke [7]. In this sense, it is important to maximize rehabilitation during this period.

Conventional rehabilitation, such as physical therapy for motor recovery and speech and language therapy for aphasia, have been widely practiced. Research suggests three main principles for post-stroke motor recovery. First, rehabilitation should begin as soon as possible since almost all impairment recovery occurs in the first three months after a stroke. *Biernaskie et al.* [41] confirmed in preclinical tests that a sensitive window of marked plasticity starts about five days after ischemic stroke. If therapy is started in this window, motor recovery is superior to when the therapy of the same dose and duration is started later (about 14 and 30 days after the stroke). In patients, the post-stroke sensitivity window starts in the first ten days following an injury and lasts for three to six months [7], [42]. It is unclear what causes these spontaneous and normal logarithmic variations in impairment during the initial months following a stroke. Nonetheless, in the first ten days following injury, there has been evidence of increased activity in the contralesional hemisphere in patients, followed by an increase in the ipsilesional one [43]. This sequential activation has been linked to improvements in motor function. Second, therapy is more beneficial if it is highly intensive and over a long period of time [44]. Third, rehabilitation is essential for significant recovery from impairment [45], [46]. Further, tasks and exercises should target objectives pertinent to patients' needs [44].

Rehabilitation motor improvements are usually measured with the help of indicators such as the Fugl-Meyer Assessment (FMA) scale. It is the most used index to assess the level of motor impairment of post-stroke patients and its evolution throughout the rehabilitation process, with higher scores indicating lower impairment. It is divided into five domains: motor function, sensory function, balance, range of motion, and joint pain. For each item, the subject can get a score from 0-2, where a zero score is given if the subject cannot do the task, a score of one represents a task that was done partially, and a score of two is given when the task was performed entirely. The maximum possible score on the Fugl-Meyer scale is 226, which corresponds to full sensory-motor recovery. However, it is common to assess all domains separately and only assess upper or lower extremity motor function [47]–[49].
One of the limitations of the FMA index is that most patients remain on the intermediate level score for a long time since the score scale is limited and the possibility of reaching a plateau in both the sensory and balance domains [48], [50]. Therefore, other complementary indicators were developed and are used in the clinics alongside the FMA. Two of them are the Wolf Motor Function Test (WMFT), a time-based activity indicator that evaluates the performance of tasks, where higher scores indicate better function [51] and the motor status score (MSS), which measures shoulder, elbow, wrist, hand, and finger movements and impairment [52]. Other upper-limb assessment tools include the Action Research Arm Test (ARAT) and the Box and Block Test (BBT). ARAT offers a comprehensive evaluation of the upper limbs since it takes into account both the proximal arm and hand and evaluates the ability to manipulate and transfer both smaller and larger objects [53]. BBT measures unilateral gross manual dexterity and is frequently used for both children and adults. The goal of this test is to transfer the greatest number of blocks possible in 60 seconds from one compartment of a box to another compartment of similar size [54].

Conventional therapy requires a professional therapist to perform repetitive movements, training the affected limb. This can be very time consuming for the patient and therapist, as well as labor intensive,

requiring one-on-one therapist–patient interactions for highly impaired individuals [55]. However, modern technological advancements have expanded the methods for post-stroke rehabilitation in addition to physiotherapy.

2.3. Robotic Rehabilitation

Robotic rehabilitation is an innovative technology that has been of particular interest, being studied as a way to reduce motor impairment [56]. This is because robotic devices can objectively measure biomechanical limb functions, e.g., range of motion, the torque of the user's movement, and therefore the user's performance and progress through their embedded sensors. Additionally, they may be able to treat people without the therapist's presence, enabling more frequent treatment and potentially reducing costs. The rehabilitation process can even be reproducible, enabling specific task-training procedures to be applied simultaneously. Finally, robotic rehabilitation devices have the advantage of increasing training duration and intensity compared to conventional therapy, reaching more than 1000 movements compared to 45 of conventional stroke therapy [9].

In the 1990s, the first robotic device was introduced for post-stroke upper limb rehabilitation. This device was the MIT-Manus (Figure 2.2), designed to assist planar reaching movements [57]. Many rehabilitation robots have been developed since then. While some randomized controlled trials have shown that robot-assisted therapy is just as effective as conventional therapy, most published works have never been clinically assessed or have only undergone pilot studies with a small number of patients.

Robotic rehabilitation devices can be categorized on their mechanical structure: end-effector (EE) based and exoskeleton-based systems [58]. In end-effector-based devices, the patient's upper limb extremity (hand or wrist) is only attached to the most distal part of the robot (i.e., end effector). Despite these devices granting an easy setup, it is impossible to control the proximal segments of the patient's upper limb, potentially resulting in undesired compensatory movements. An example of an end-effector robot is the MIT Manus (Figure 2.2). This device provides two translational degrees of freedom (DoF) for elbow and forearm motion and an additional three DoF for wrist motion [59].

Figure 2.2 *- MIT-Manus's end-effector rehabilitation robot from Interactive Motion Technologies, Cambridge, MA. Figure taken from [55].*

Exoskeleton devices, on the other hand, are more complex structures that resemble the patient's upper limb structure. They enable simultaneous and independent control of numerous robot joints, directly influencing the position of the corresponding joints in the patient's arm. As a result, these devices can provide more sophisticated movements and rehabilitation exercises. However, due to this complexity, they tend to have a very high manufacturing and acquisition cost which may even prevent more institutions from implementing them in their rehabilitation plans. This complexity also makes them not very user-friendly, requiring a process of getting used to the equipment and its functionalities by the therapist. Additionally, since they are adjusted to custom fit each patient, this makes it take longer to prepare and place the user inside them [58], [60]. Nonetheless, as more research is done, more individuals can benefit from this promising technology.

2.3.1. Exoskeleton Robots

Recently, exoskeleton robots have gained high interest in robotic therapy research. [61]. These mechanical structures are connected to the human body in multiple locations so that the rotation axis of the robot joints is aligned with the rotation joints of the wearer [62]. Therefore, these devices can cover an extensive range of motion, and any portion of the specific limb or body part can be targeted for training.
Based on the supported body part, exoskeletons can be divided into upper or lower limb systems, integrated upper and lower limb systems, and specific joint muscle strength support systems. The upper limb systems involve the chest, head, back, and shoulders while the lower limb systems involve the thighs, lower legs, and hips. [63].

The exoskeleton robots are usually composed of active and passive joints. Active joints are actuated through the help of an external source, such as electric motors or hydraulic cylinders, giving the user assistance in performing the desired movements. On the other hand, passive joints do not have a power source and can only be moved passively by the user's movement or adjusted manually, e.g., to tailor the device to the user's needs [63]. Additionally, several control techniques have been used in terms of the movement of an upper limb exoskeleton. There are three ways the exoskeleton can function: passively (robot-driven), actively (patient-driven), and challenge-driven (robot resists the applied force). It is a robot-driven control method

or passive approach if the robotic device is active and only guides the patient in the therapy session. In contrast, a patient-driven control or active method focuses on the patient's initiative muscular activity and aids in movement according to the patient's intention, where the motion and the interaction force are controlled by the patient's voluntary effort. Finally, the robot can also resist patient movement to make it more challenging for the patient, applying a challenge-based control strategy [64].

There are several available rehabilitation devices for the upper limb (Fig 2.3). One of the more sophisticated devices is the ARMin rehabilitation robot, developed in ETH Zurich, with six active DoF and weight support capabilities for stroke rehabilitation. Weigh support is used to help the patient during the rehabilitation session, allowing them to perform the movements more easily by actively compensating for friction and gravity. It can be adjusted, giving help depending on the patient's impairment and the training objective.
Examples of other devices include the ArmeoPower (Hocoma AG, Switzerland), a 6 DoF exoskeleton similar to ARMin that embraces the whole arm, from shoulder to hand, and is able to provide arm weight support, counterbalancing the weight of the patient's arm to make it more challenging to perform the designated tasks [65]. CADEN-7 is another active assistive exoskeleton, which has the particularity of having the actuators at the back, transmitting the force/torque via cables instead of the most common approach of the actuators being placed locally at the joints [66]. The Wilmington Robotic Exoskeleton (WREX) is a passive orthosis with two links and four DoF that can be mounted on a person's jacket or wheelchair. It uses linear elastic elements that balance the effects of gravity to help with neuromuscular disabilities [67]. RUPERT IV is a wearable upper extremity that is lightweight and thus very portable. It is intended to assist in repetitive therapy tasks related to ADLs and can be worn while standing or sitting [68].

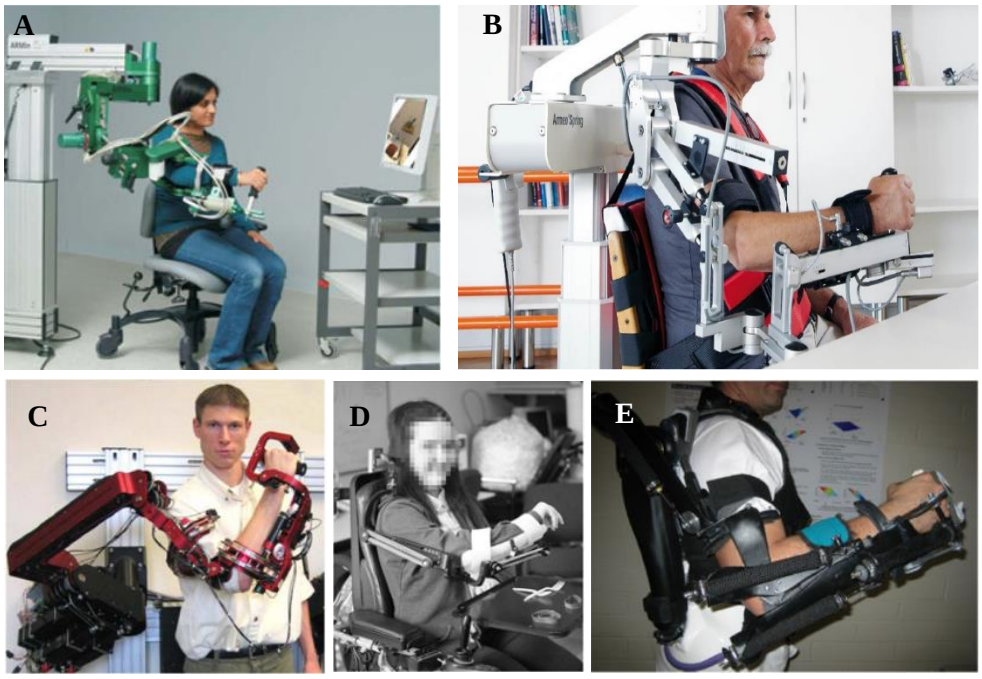

Figure 2.3 *- Examples of upper limb rehabilitation robots: (A) ARMin III rehabilitation robot* [109], *(B) ArmeoSpring from Hocoma, Switzerland* [65], *(C) Cable-actuated CADEN-7 exoskeleton* [66], *(D) Passive arm exoskeleton WREX* [110], *(E) Wearable upper extremity exoskeleton RUPERT IV* [68].

Although most upper limb rehabilitation exoskeletons allow for rehabilitation from the shoulder to the

wrist, they do not allow movements at the hand level. While some hand rehabilitation devices have been developed for finger motion [69], a complete upper limb exoskeleton with actuated DoF from the shoulder to the finger joints can allow for more complete rehabilitation exercises.

2.4. Virtual Reality

With Virtual Reality, users are surrounded and can interact with a computer-generated world where both realistic and unrealistic events can occur. It is a new technology, first developed in the 20th century. However, it is only in the early 21st century that it has received more attention and, therefore, more investment and applications in various areas, Figure 2.4. Nowadays, VR is primarily used for entertainment, mainly for playing video games and social interactions at the virtual level. Nonetheless, more applications can be integrated since VR is a low-cost but safe technology.
Other applications include educational purposes, where a realistic but controlled environment can be simulated where, for example, students can perform laboratory experiments, having direct feedback on the outcome without any risk of danger to them or their peers [70]. This is also the case for military simulations and training [71], as well as for pilots [72] or medical training [73], where users can develop their skills without the risk of failure [74]. In science and psychology, virtual reality has been used as a therapeutic intervention [75]. Exposure therapy is applied to help treat anxiety disorders such as post-traumatic stress disorder and phobias. In rehabilitation, VR has been used since the 2000s, mainly for helping with Alzheimer's disease [76] and loss of motor function.

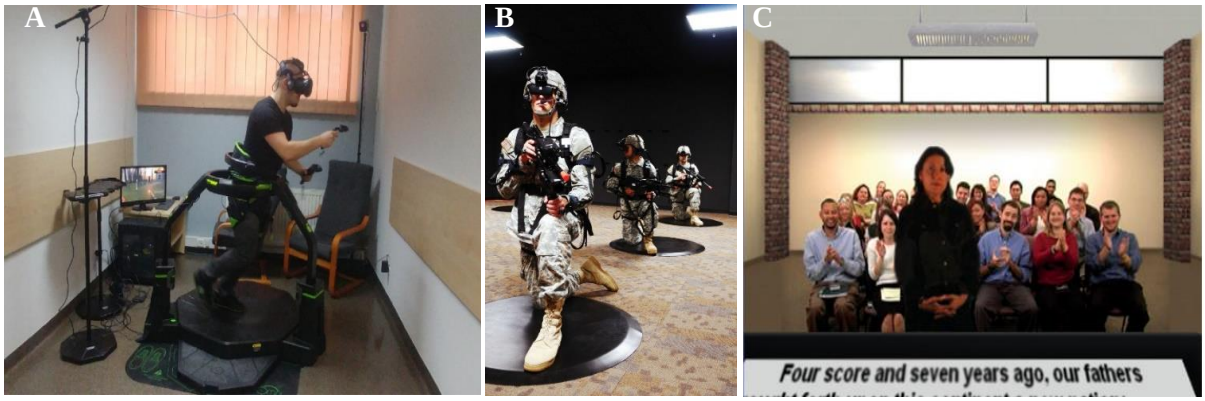

Figure 2.4 *- Various applications of VR: (A) for gaming and entertainment purposes* [111], *(B) for military training* [71] *(C) fighting fear of public speaking through the help of VR* [75].

The term Extended Reality (XR) refers to all immersive technologies that expand the reality that a person perceives by blending the virtual and real worlds. It includes the concepts of mixed reality (MR), augmented reality (AR), and virtual reality. Augmented reality modifies how the real world is perceived by replacing physical items with virtual ones. It is mainly used through the cameras of smartphones and tablets. Mixed reality, also referred to as hybrid reality, allows the user to interact with both worlds. It goes beyond AR, where the virtual and physical worlds coexist. With mixed reality, it is possible to move seamlessly between the real world and a virtual setting simultaneously [77].

Virtual reality motion sickness, also known as cybersickness, is one of the major things that impede the

growth of VR technology. Some symptoms are general discomfort, blurred vision, headache, and vertigo. [78]. It occurs when there is a conflict between the vestibular motion cues that the brain perceives and the visual motion information from the VR environment. The refresh rate can also have an impact on the occurrence of motion sickness since often the refresh rate of the VR devices is slower than what the brain processes, causing discord between the processing rate and the refresh rate. This condition reduces the immersion and interactivity of VR technology and affects the user's health [79], [80].

Wood et al. [89] noted a high degree of realism as a vital structural element of video games for players. To create a realistic virtual environment, a consensus must exist between proprioceptive information, the person's sense of position and motion of body parts, and visual feedback. If this is the case, the VE displays the movements naturally, giving the user the impression that they are physically present in the virtual environment—a feeling known as presence [81]. Furthermore, the user can control an avatar, which may also lead to a virtual embodiment, a condition where the user views the avatar's body parts as substitutes of their own, leading to a sensation of ownership [82]. If all these factors are present, we refer to it as immersive virtual reality (IVR). It is important to note that better motor performance has been linked to a strong sense of bodily ownership of an avatar in immersive VR. *Wenk et al.* [18], [83] further demonstrated that visualizing an avatar through an immersive VR HMD rather than a computer screen facilitates motor performance and increases user motivation and body ownership over the avatar.

VR can range from being non-immersive to being totally immersive, depending on the degree to which the user is separated from their physical surroundings when interacting with the virtual environment. In non-immersive reality, users interact with a computer-generated environment but are always aware of their physical environment. These systems rely on a computer or video game console, display, and input devices such as keyboards, mice, and controllers. Non-immersive VR systems can give users a first-person perspective that they can associate with their virtual avatar to increase the level of immersion. On the other hand, immersive reality provides the user with a feeling of being in the VE [84].

The main goal of immersive VR is to give the user a sense of presence, the illusion of being in the rendered place, which makes them more likely to interact with the stimuli and the virtual environment, where the more accurately the body motions are recreated and matched, the more immersive the environment is [15], [85]. The most common form of interaction with IVR is through the use of a head-mounted display (HMD).

However, the real world is very complex. Therefore, it is crucial to appeal to as many senses as possible when creating and using a VE. One such example is using headphones to give the user a sense of sound or incorporating haptic feedback to simulate touch. However, this can increase the cost of VR systems and reduce portability.

There are many HMDs commercially available. Currently, among the most used HMDs for virtual reality, there is the Oculus Quest 2 (Meta, LLC, Menlo Park, CA, USA) and HTC Vive PRO (HTC Vive, HTC, Taiwan & Valve, USA). Both enable tracking the user with six DOF, built-in speakers, and an OLED screen for high display resolution [12], [76], [86]. Recently, other HMDs have also been gaining interest, such as the Varjo XR-3, due to its ability to provide extended reality with a high level of quality and definition and a field of view of 115º, being able to switch between XR, AR, and VR. It also has the ability to monitor eye and hand movement and combines a LiDAR sensor and stereo RGB video feed to blend virtual elements

with real ones [87].

2.4.1. Virtual Reality in Rehabilitation

The use of more immersive VR in motor training environments has been encouraged by recent reviews [16], [88]. Thanks to the ability to create motivating task-oriented exercises, games have been used to study different outcomes of using VR for motor rehabilitation. This is the case in *Lee et al.* [89], where twelve people after a stroke had to play five mini-games involving upper limb movements in 3D space, resulting in improved motor performance and high patient satisfaction. Although only a few studies have investigated the use of HMD for motor neurorehabilitation in the last ten years, thanks to studies such as *Christou et al.* [90], *Weber et al.* [91], and *Gobron et al.* [92], in which HMD was well tolerated and without any adverse effects recorded, it is possible that this technology will be increasingly used and implemented in this type of rehabilitation.

By combining virtual reality with robotic therapy, many benefits can arise. Through the enhancement of enjoyment and gamification, i.e., adding game-based elements such as time activities and rewards, VR can stimulate user engagement and enhance training duration and task repetition [93], [94]. Therefore, it can transform repetitive and monotonous tasks prevenient from conventional rehabilitation procedures into more motivating training that ultimately improves the user rehabilitation process [10]. An important factor that helps users feel motivated is goals at different levels, e.g., reaching a goal after one minute, in the middle of the game, and at the end, and interaction features, challenging the player to the edge of their ability [95], [96].
Another advantage of virtual environments is the possibility to manipulate feedback safely, e.g., haptic or auditory, the duration and intensity of the exercises, as well as the flexibility to switch among different tasks, adapting to each need and promoting neuroplasticity. It also enables people to engage in activities that feel and look similar to real-world objects and events, which can help them accomplish specific ADLs[12]–[14].

2.4.2. Robot Visualization & Digital Twins

Interaction with the virtual environment remains challenging. The VE must be designed to promote impaired limb movement of people after a stroke. However, the best way to motivate the patient to perform the desired tasks and movements is still unknown.
The majority of users in the current IVR interact with the VE using controllers rather than assistive robotic devices [18]–[21]. Additionally, the VE hardly ever displays the assisting robot, leading to a discrepancy between the user's perception and what they see.

Digital twins have been gaining interest across many industries due to their ability to virtually replicate a living or non-physical entity and simulate their features [97]. They are a promising concept that has become the focus of interest in the industry and, in recent years, in the healthcare sector due to the promising ability to analyze systems remotely in real-time, prevent problems before they occur, and provide customization and the ability to test products in VEs even before they are built. The concept of DT first surfaced in 2003 when *Grieves et al.* [98] introduced the concept by proposing an early version of the DT with three components: physical product, virtual product, and their connections, (Figure 2.5). Since then, the DT

enabling technologies have grown exponentially.

Currently, DTs are mostly developed and implemented to validate designs through the use of synthetic data, immersive technologies, and AI [99]. With the simulation system is possible to generate the product and perform the necessary significantly reducing the cost of the investigation. Therefore, it is used in many industries such as aerospace engineering, car manufacturing, and healthcare [100]. For example, *Tuegel et al.* [101] applied a DT to predict the structural life of the aircraft and reported that it could facilitate the management of aircraft service life. Another example is Nvidia's Omniverse3, a 3D simulation and design collaboration platform [102]. It offers simulation tools that are being used to test robotic tasks in VR before implementation, enabling the understanding of outcomes without jeopardizing the production process.

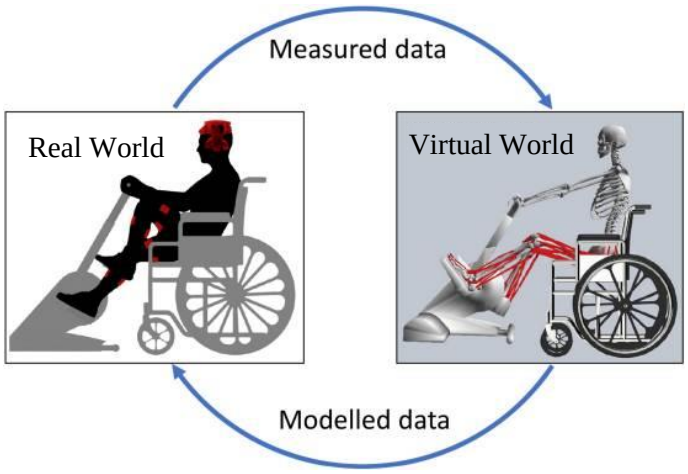

Figure 2.5 *- Model of a digital twin. Figure adapted from* [103].

Nonetheless, there are some early applications of DT in the healthcare sector. One of these examples is The Living Heart Project [104] which models the cardiovascular system of a particular patient's heart and turns it into a DT with all the medical data. This enables the reconstruction of the patient's vascular system and therefore study and find the best-fitting treatment option without incurring any risks.

However, not much research has been done on using DTs in upper limb robotic rehabilitation, especially when combined with VR, suggesting that DTs in medical care are still in their infancy. Thus, a systematic review was conducted on the use of DT in the healthcare sector, more specifically, to enhance upper extremity motor recovery in stroke survivors.

In the systematic literature review, the PubMed, IEEE Explorer, and Web of Science Core Collection databases were used. The following terms were used in advanced search: robotic rehabilitation and digital twin; assistive robot and virtual-reality and visualization and upper limb; assistive robots and digital twin; and robotic rehabilitation and digital twin and upper limb. The query yielded a total of 42 results, 26 without duplicated papers. After removing review papers and the ones that were not relevant to the subject, two publications were found [86], [105]. The word "stroke" was not included in the research terms as it did not show any different or relevant results. It is also important to note, as seen in Figure 2.6, that when searching for the keyword "digital twin," all papers ranged from 2019-2022, indicating that this subject is still very

recent and therefore explaining why there were so few results found.

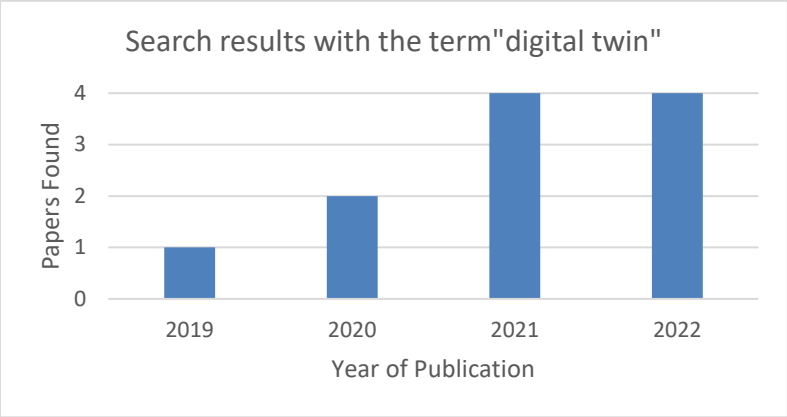

Figure 2.6 *- Histogram of the number of papers found in the PubMed, IEEE Explorer, and Web of Science Core Collection databases per year of publication.*

In the paper published by *Topini et al.* [105], a digital twin of the pre-existing hand exoskeleton developed by the researchers at UNIFI DIEF and intended for patients with restricted hand mobility was developed. It was designed to give the user visual cues during rehabilitation activities and sensory feedback from the VR environment. The kinematics of the real device was replicated through virtual components (i.e., connections and joints) that physically mimic the mechanical characteristics of the real parts. Each virtual exoskeleton's finger mechanism was driven with a virtual motor, acting the same as the real ones. As a result, the exoskeleton helped the patient move by providing force feedback and following a calculated reference value within the VR, giving the user a sense of force feedback whenever a virtual object was grasped.

In *Wenk et al.* [86], some preliminary research was conducted where an immersive VR system with an HMD and a first-person perspective avatar plus a digital twin of the rehabilitation robot was developed. The participants performed a path-tracing task with their right hand in four conditions: invisible and visible robot, both with and without assistance. Through a series of questionnaires, it was reported that the robot visualization did not affect the user's rehabilitation process in factors such as performance, motivation, presence, and task performance, thus indicating no disadvantage of not reproducing robotic devices in VEs when using HMDs.

It is important to note that both studies did not use stroke patients but only studied a small group of healthy patients (one and twenty-eight, respectively). This shows that there is still a need to better understand the possible effect of digital twins and how they can improve rehabilitation processes. Nevertheless, DT has been recognized as a promising technology, and it is anticipated that DTs will thrive in the upcoming years and bring a revolution in several industry sectors due to consumer demand for online monitoring, greater flexibility, and individualized services [106].

3. Methods

This chapter provides a detailed description of the methods and materials used in this project. This work was divided into two different parts. In the first one, a hand module was integrated in the six DoF upper limb rehabilitation robot ARMin (SMS-lab, ETH Zurich, Switzerland). Second, a digital twin of ARMin was developed in Virtual Reality.

3.1. Integration of the new Hand Module

With the objective of creating a more realistic yet functional interaction with the VE, the PRIDE hand module, developed by *Rätz et al.* [1] and with fine haptic render capabilities, was used, Figure 3.1. This device is able to offer, with an effortless setup, a 180º range of motion for finger flexion and extension, while giving a comfortable grasp to the user. Size-specific handles (small, small-medium, medium-large, large) can be placed and exchanged to fit the size of the user's hand.

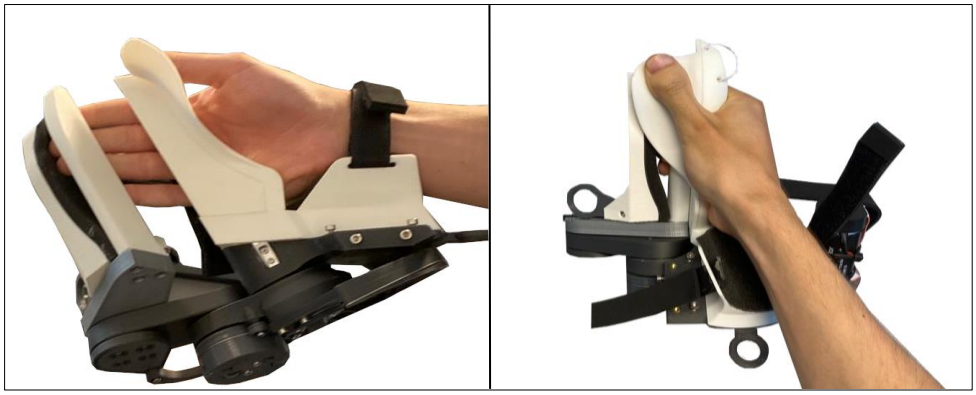

Figure 3.1 *- clinical-driven Palmar RehabilitatIon Device (PRIDE)* [1] *integrated in the ARMin upper limb rehabilitation robot.*

The aim of this novel hand module was to be integrated into the ARMin upper limb rehabilitation robot, with six actuated DoFs. These DoFs include horizontal shoulder abduction/adduction, shoulder elevation, interior/exterior shoulder rotation, elbow flexion/extension, forearm pronation/supination, and wrist flexion/extension, Figure 3.2. It is equipped with optical incremental Maxon MR encoders at each joint (1000 impulses per rotation). It can also be adjusted to the anatomical characteristics of each patient by changing the exoskeleton length settings for the arm length, forearm length, and shoulder angle. These three adjustment points will be referred to as passive joints. Additionally, the hand length can also be adjusted, as well as ARMin's height since its column can move up and down. The robot can also be used for left and right arm training.

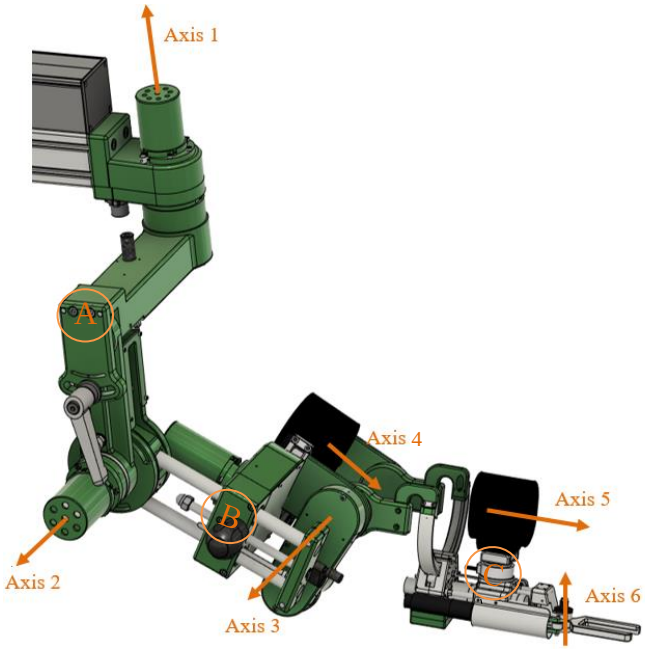

Figure 3.2 *- ARMin upper limb rehabilitation robot CAD model with six actuated DoF and their respective axis: axis 1 - horizontal shoulder abduction/adduction; axis 2 – shoulder elevation; axis 3 – interior/exterior shoulder rotation; axis 4 – elbow flexion/extension; axis 5 – forearm pro/supination; axis 6 – wrist flexion/extension; and three passive joints, A-C, that can be manually adjusted to the anatomical characteristics of each patient. Additionally, the three passive DoFs that enable adjusting to each patient's anatomical characteristics are also represented: A–arm length, B - forearm length, and C – shoulder angle.*

The connection of the previous EE, i.e., the final part of the robot that interacts with the environment, with ARMin was made through four different parts and a force/torque sensor (Figure 3.3). The FTD-Mini-45 SI-580-20 (Schunk Group, Heuchelheim, Germany) force/torque sensor that measured the interaction forces and torques between the hand of the user and the robot was connected to part 1 – Figure 3.3 (user handle, EE) by screwing in six M3 screws. Next, the sensor connected to a round adapter plate (part 2 – Figure 3.3) via six M3 screws, which subsequently extended into a cylindrical shape. The connection to the extremity of the exoskeleton was made through a third piece, similar to a regular parallelepiped with two ledges (part 3 – Figure 3.3), that fitted into this same end. This fitting allowed the piece to slide across the extremity of the exoskeleton and thus adjust the distance from the forearm to the fingertips. The second part connected to part 3 via a pin and an M8 screw, which ran from the inside of the cylindrical part to the fourth and last piece, part 4 – Figure 3.3. Finally, part 4 was located underneath ARMin's extremity, held in place by the same M8 screw and pin.

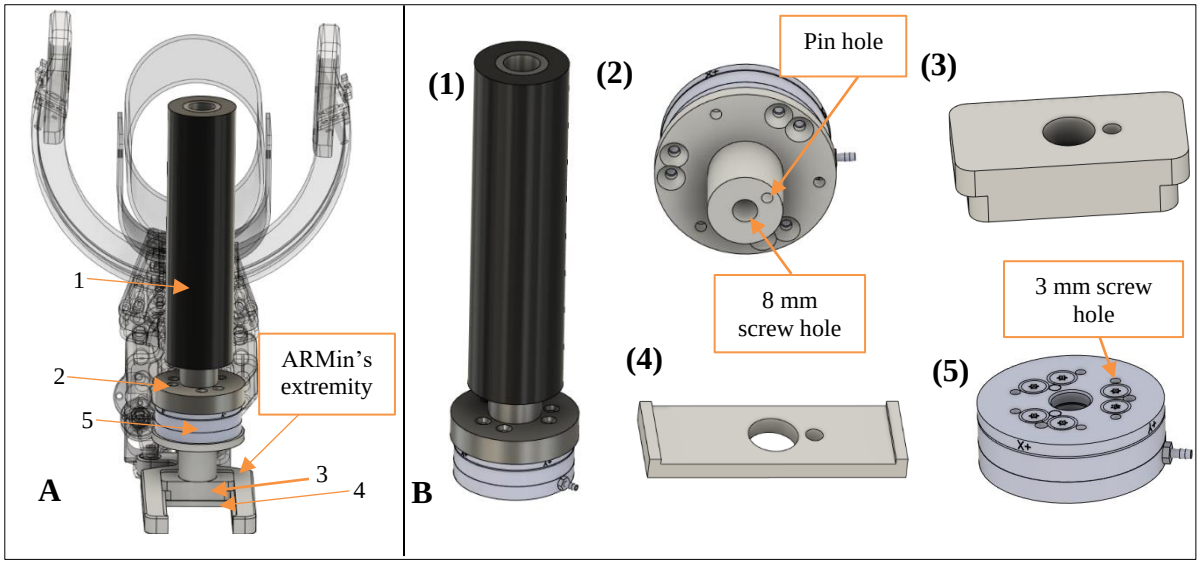

Figure 3.3 *- (A) CAD Model of the previous ARMin end-effector and (B) the parts that made the connection between this end-effector (1) and the extremity of the robot: (2) round adapter plate that subsequently extends into a cylindrical shape and that connects to the force/torque sensor in the same way as the EE, through six M3 screws; (3) one of the two parts that connect directly to the end of the exoskeleton. It slides across the extremity allowing to adjust the distance from the forearm to the fingertips; (4) the second part directly attached to the exoskeleton, connecting to the other parts through the M8 screw and a pin; (5) FTD-Mini-45 SI-580-20 force/torque sensor.*

However, users only interacted with the previous EE by grasping it with a closed hand. Although it was possible to perform rehabilitation exercises at the arm level, these were always limited to the level of the hand, which was permanently closed. Therefore, it was impossible to perform any grasping movements. In a survey conducted by *Rätz et al.* [1], the therapists stated that grasping is one of the most used movements during ADLs and, therefore, is an essential exercise activity. Consequently, it was important to make this type of movement possible in rehabilitation exercises. Thus, trying to minimize changes to the structure and parts of the exoskeleton, four parts were designed in Fusion360 version 2.0.13881 (Autodesk Inc., California, USA) and 3D printed using the Prusa i3 MK3S printers. The default printing settings were infill = 20%, solid wall = 1.0 mm, and layer thickness = 0.15 mm.

3.1.1. Top Part

Several requirements had to be met to integrate this new hand module (Figure 3.4). The most critical part was the one that allowed us to make the connection between the new hand module and the force/torque sensor. Firstly, (1) the height of the hand with respect to the lower arm was considered, as placing the hand higher or lower than the arm would cause physical load in the hand or wrist and therefore should be at the natural resting position. Adding to that, the entire arm must follow the same axis, including the hand. However, PRIDE was made with a 25º angle since it was designed considering the cylindrical hand grasp. This characteristic comes from the angle that the human hand makes when grasping a cylindrical object, from the metacarpophalangeal joint (MCP) of the index finger to the base of the hypothenar eminence (Fig 3.4) [1]. Therefore, (2) this angle needed to be counterbalanced so the user's hand would be in the neutral position.

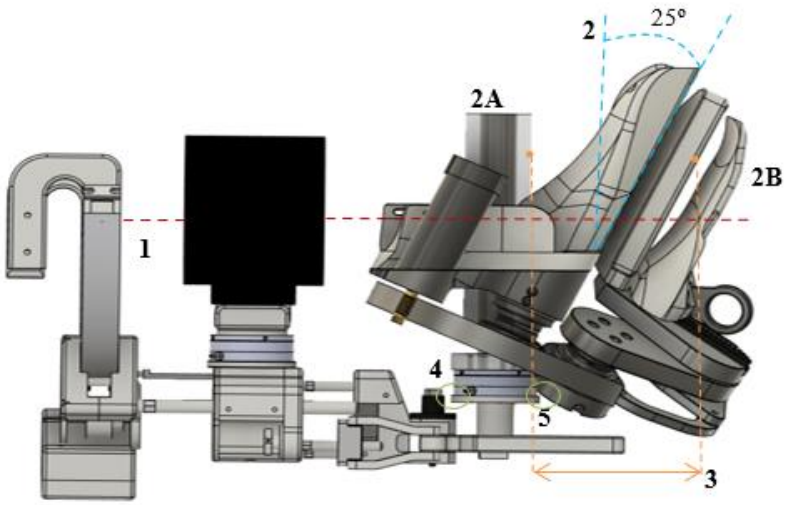

Figure 3.4 *- Representation of all parameters to be considered in the design and integration of the top part and consequently the hand module. (1) It needed to follow the same axis as the arm, so the hand would be at the neutral position and not cause any physical load. (2) 25° angle characteristic of the cylindrical grasp and which needed to be counterbalanced so that the person's hand would be in a neutral position, following axis (1). (3) it was important not to change the EE position, despite the new hand module: 2B EE being in a different position when compared to the previous 2A. (4) Limitation of space for the integration of the hand module by the hall sensor, constraining how far back it could be moved and (5) in terms of height and rotation, since if PRIDE was too low, it would collide with other parts and prevent the full 180° movement.*

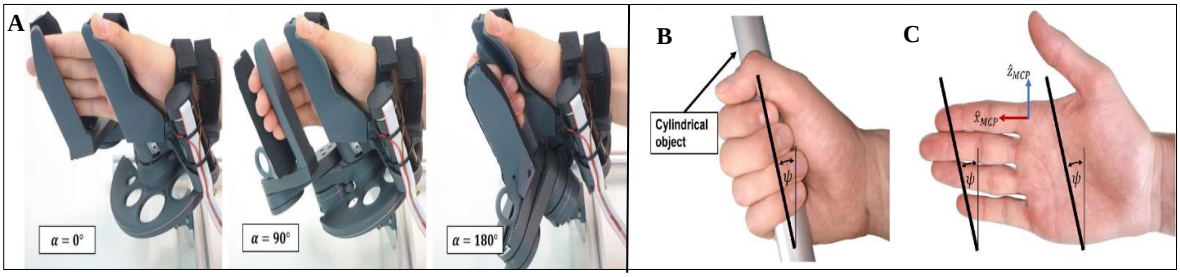

Figure 3.5 *- Characteristics of PRIDE hand module. (A) Hand movement sequence from full finger extension to 180º flexion. (B) Illustration of the cylinder angle ψ = 25° while the hand encloses a cylindrical object, and (C) with an open hand, as well as the line connecting the fingertips from index to little finger. Figure adapted from* [1].

Another important factor was the length of the forearm. Since ARMin has adjustable arm lengths to adapt to each patient, (3) it was important not to change the previous EE position since this difference would change the percentile of people who could use the robot for rehabilitation.

Furthermore, the hand module was limited in terms of space. On the one hand, (4) a hall sensor constricted how far back the hand module could be moved. On the other hand, (5) it was limited in height since reducing it too much would block the hand module from performing the full range of motion, thus defeating its purpose. Finally, (6) this part had to be strong enough to support the weight of the hand module, keeping it stable, as it was heavier than the previous end-effector, weighing 920g compared to the 120g of the previous end-effector.

With all this in mind, the part was designed, and 3D printed using carbon fiber-infused nylon as the material since it has a high strength-to-weight ratio. Fillets and chamfers were added to reduce the stress concentration of the edges of the parts.

3.1.2. Connecting the force/torque sensor to ARMin

In order to make the connection between the force/torque sensor and ARMin, three more parts were designed and fabricated. It was important to take some things into account. First, (1) the height of the hand, as mentioned earlier, had to be considered. However, due to the greater complexity and constraints of the top part, these three parts could be more easily changed. Therefore, the part that would connect the force/torque sensor to ARMin, previously designed as the circular and cylindrical part (Figure 3.2 - component 3), was designed with the top part in mind.
Two other pieces were developed to take advantage of the part located at the end of the exoskeleton (ARMin's extremity) and continue to allow adjustment of the distance from the forearm to the fingertips. These pieces had the (2) requirement to fit into the end of the exoskeleton, thus allowing this same adjustment.
Finally, (3) the pieces needed to remain fixed and stable. Hence, the first part was printed in 100% filled Polylactic acid (PLA) to add more robustness. For the other two, also printed in PLA, two holes for 4 mm screws were added, which, together with a nut, allowed the pieces to be fixed and connected to the exoskeleton. For these three parts, fillets and chamfers were added, as was done with the top part, to reduce the stress concentration of the edges.

3.2. ARMin Visualization

Each joint was addressed separately to create a digital twin of the seven active and three passive DoF robot exoskeleton. First, each 3D model of the joint was imported into Blender version 3.2.2, (Blender Organization, Amsterdam, Netherlands), a free and open-source 3D computer graphics software tool. Here it was possible to set the pivot point, which corresponded to the center of rotation of that joint in the case of the seven active and the passive shoulder angle joints and the center of the translation in the case of the other two passive joints, Figure 3.6. Finally, the axes were adjusted so that the rotation/translation axis on which the joints moved was in the desired direction to emulate the behavior of the real robot.

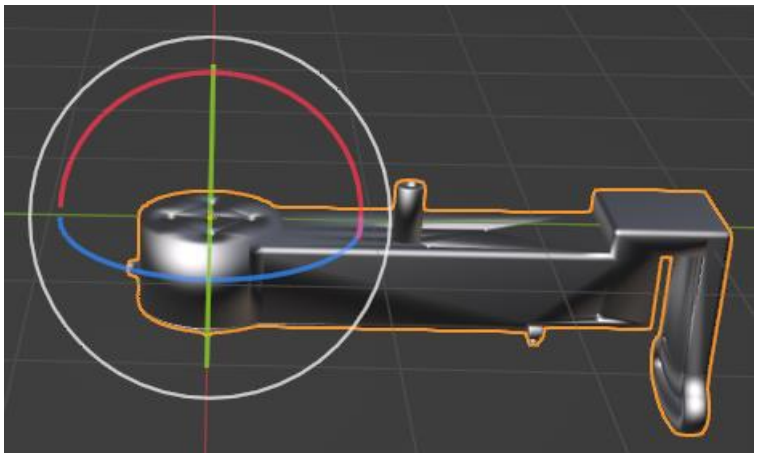

Figure 3.6 - *Definition of the pivot point, the center of the translation/rotation of the respective joint, in Blender.*

Afterward, each joint was imported into Unity (Unity Technologies, California, USA), a cross-platform game engine often used for the creation of three-dimensional (3D) and two-dimensional (2D) games that

provide realistic behavior for objects with built-in physics. The robot's base was first imported by creating a project through Unity Editor 2021.3.2f and setting a scene with a floor and four walls. Next, the first joint was placed manually, as precisely as possible, in its actual location. To establish a joint relation, the rigid body property was added to the base frame and to the placed joint. However, this property causes the position of the respective object, in this case, the first joint and the base frame, to be controlled through physical simulations. This could create some conflicts when all joints are in place since each joint would be affected by the forces from the other joints, creating unwanted and unrealistic movements. Since the goal was that the model would only precisely move when the real robot did, the "is kinematic" property box was checked (Figure 3.7). With this property activated, the objects would not react to collisions or forces and could only be moved with a script. Finally, a joint relation was added, “configurable joint”. Although this property allows much customization, almost all the parameters were left as default, only changing the connected body to, as the name indicates, the body to which the joint was connected, in this case, ARMin’s base frame. Another parameter that was changed was the movement of the joint, which was restricted so that it only rotated on a single axis, mimicking its actual behavior. This process was then repeated for all rotational joints.

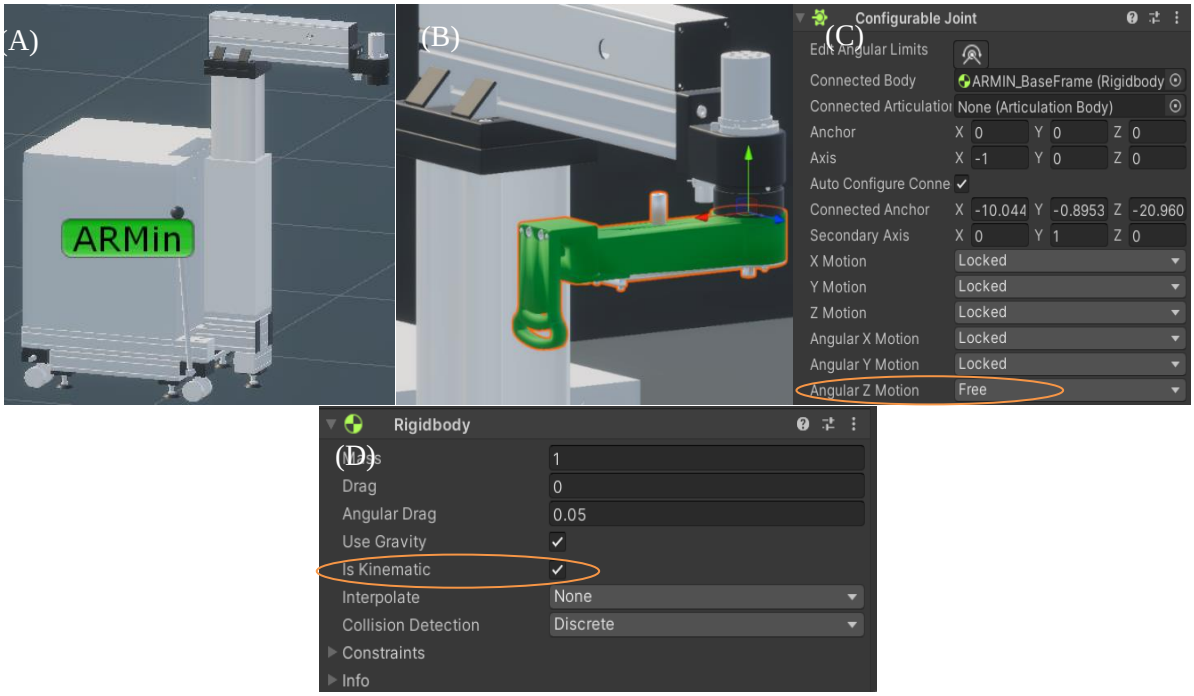

Figure 3.7 *- Process of implementation of every joint in Unity. Once the connecting part (A) and the joint (B) are manually placed in the desired position, a configurable joint (C) is added, where the connected body (the base frame (A) in this case) is defined and the axis under which the joint moves, as well as the rigid body characteristic and the “is kinematic” property (D).*

The next important step was to adjust the hierarchy of the different components. Unity uses the concept of parent-child hierarchies (parenting), to group components (GameObjects) together. This means that by placing one component inside another in the hierarchy, it becomes the child, and the component above it is the parent. Thus, the children become dependent on the parent, inheriting its movement and rotation.

Through this relationship, it is possible to create a chain movement, where if the first joint moves, all the other joints will move with it. With this concept in mind, the ARMin hierarchy was configured, as seen in Figure 3.8.

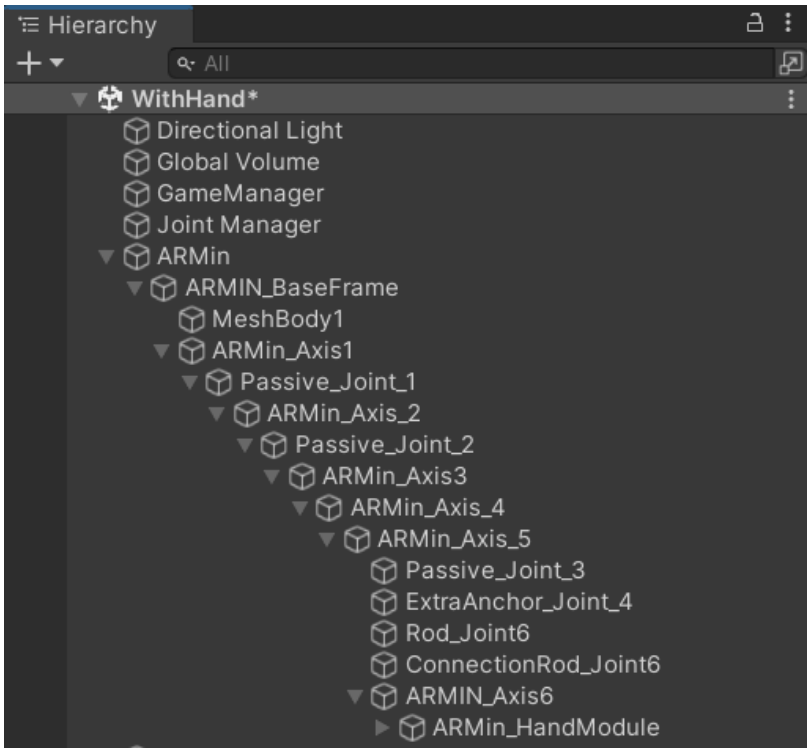

Figure 3.8 *- ARMin's hierarchy in Unity. It is possible to see many parent-child hierarchies. For example, "ARMin Axis_3" is the parent of "ARMin_Axis_4", who is the parent of "ARMin_Axis_5" who subsequently has more children. This means that the movement and rotation of "ARMin_Axis_3" will also affect "ARMin_Axis_4" and its children (from "ARMin_Axis_5" to "ARMin_Hand_Module").*

With the hierarchy fully established, each joint was configured to behave exactly like the real exoskeleton. The ARMin kinematics model, with all the information regarding the joints' angles and respective coordinates, was developed at ETH Zurich and was available in Simulink, a modeling and simulation tool incorporated in MATLAB (Mathworks Inc., Massachusetts, USA).

To get this data in real-time in the virtual environment, various scripts were developed using the C# programming language and the User Datagram Protocol (UDP), a communication protocol used to send messages to other hosts on an Internet Protocol (IP) network. Therefore, using UDP and a C# script, it was possible to communicate the joint's data in real-time.

To mimic the real motion, it was first necessary to position each rotational joint in the virtual environment at the position marked in the kinematic model as 0°. From this initial position, a script was developed that compared, for each joint, the angle received from the real robot with the rotated angle in which the respective joint was in the VE. If there were any differences, the virtual joint would rotate the number of degrees corresponding to that difference. This difference was calculated in every frame. For it to rotate in the desired direction, it was previously defined in Unity not only the axis at which the joint revolved but also the positive

direction of the rotation, Figure 3.9.

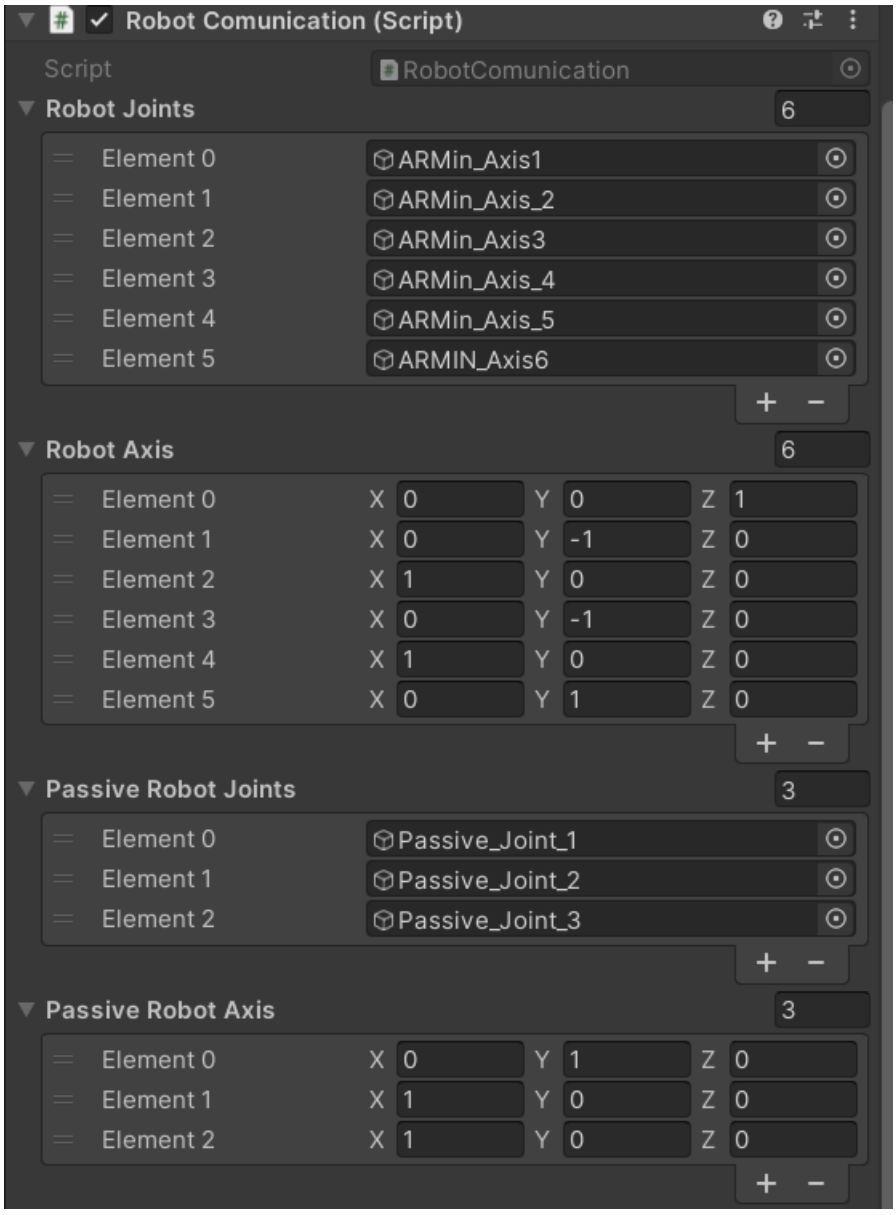

Figure 3.9 *- Assigned components of the Robot Communication script, used to get joint's data from ARMin and translate it to the VE. Each joint was assigned the movement/rotation axis, as well as the direction, with a "-" representing the counterclockwise direction.*

The process was slightly different for the translational joints, meaning the adjustable arm and forearm segments. First, it was recorded what the maximum limits of the joint were, i.e., what the maximum value the joint could take when moved fully backward (a) and when moved forward (b). These values were measured using the robot's kinematic model, obtaining the range. Then, the same logic was applied to the VE, where the joint was moved to each limit and retrieved Unity's position value in each case (values c and d). Finally, and using the remap function of the *Mathematics* package in C#, it was possible to remap the position value x of each joint linearly, between the interval [a, b], to the interval [c, d], corresponding to the

interval of the VE. That is, in the case of the adjustable arm segment, which as maximum position limits presented [0.235, 0.405] m, and [-0.715, -2.34] m in the VE, it was possible to obtain any value within the first interval and linearly remap it to the second interval, thus presenting the same position in the VE as in real life. Hence, both would be moved to their respective x value after the remapping.

The last step was to animate the hand module to behave as it does in real life. Using Blender's capabilities and with the help of the VRZone team in TU Delft, the movable parts were animated throughout the opening and closing movements. Finally, a script was created to link the data recorded by the hand module's sensors to the animation, allowing the hand module to move to the recorded angle while doing the programmed animation. To avoid blocking the user's field of view, the hand module opacity was reduced. This last step is explained in more detail in the following section. Nonetheless, the summarized workflow for creating the digital twin of ARMin is represented in Figure 3.10.

Figure 3.10 *- ARMin's digital twin development workflow.*

3.3 Virtual Reality

To incorporate virtual reality into the already developed virtual environment, an HMD was required. The HMD chosen was the Varjo-XR3 (Varjo Technologies Oy, Helsinki, Finland) due to its high resolution and AR capability that, although not going to be used in this work, could come in handy in the future, Figure 3.11.

Figure 3.11 *- ARMin upper limb rehabilitation robot with PRIDE hand module and Varjo XR-3 HMD.*

For the position and movement of the HMD to be recorded while the patient was moving the robot, two HTC base stations were used (HTC, Taiwan & Valve, USA). Due to the position differences between the digital twin and ARMin, an HTC Vive tracker was placed on the real exoskeleton to calibrate the position of the DT in the VE. The base stations register the position of this tracker. Thus, considering the relative position of the tracker on the ARMin, a reference point was placed on the DT with the same position as the tracker (Figure 3.12). Then, when starting the simulation, the DT would move so that this reference point coincides with the tracker's position. Thus, the position of the DT would be changed to the actual position of the robot, leaving both in the same position.

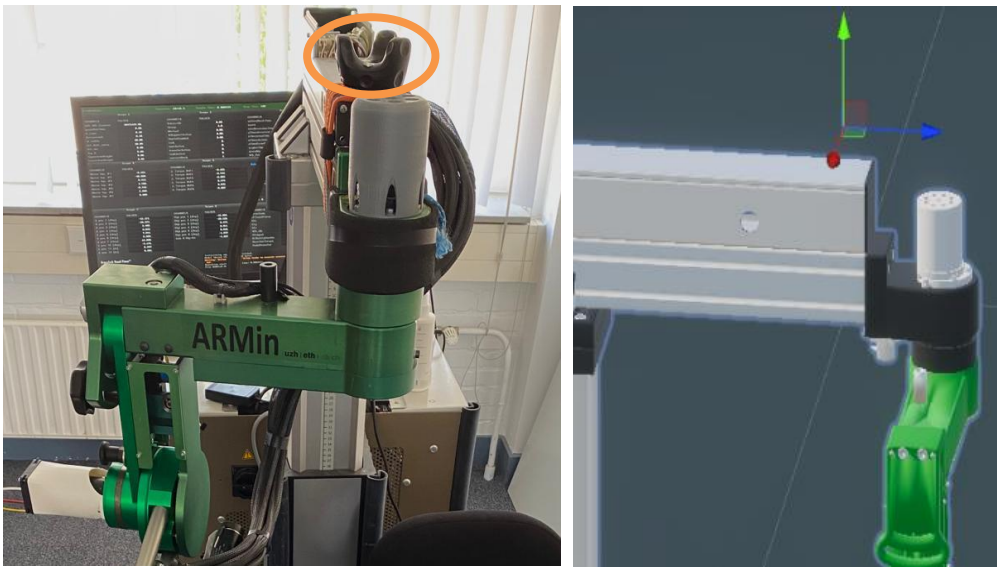

Figure 3.12 *- Positioning a tracker on top of ARMin and its reference point in the VE. Upon starting the simulation, the position of the tracker would be recorded on the VE, from which the reference point would move to that position and subsequently the entire ARMin, thus being at the same location as the real robot.*

To connect and read the base stations, the HMD, and the tracker in Unity, SteamVR was installed. The Varjo headset has a plug-in that allows it to be easily and quickly incorporated into the VE. However, due to the use of a VIVE tracker, it was found that it does not work well with this plug-in. Thus, the Open VR Loader and OpenXR plug-ins, commonly used for AR/VR development and that work together with SteamVR, were used. Another used package was the High-Definition Render Pipeline (HDRP) package, allowing for a greater definition of the objects' textures and colors. Also, with SteamVR, "Room Setup" was performed, providing data on where the ground is and indicating which orientation the HMD faces when the user is in a position to achieve the desired task.

To create a more immersive virtual reality and a sense of embodiment, but also considering time-constrains, a 3D model of a hand was added to the hand module. The chosen hand visualization model was a pre-existing glove, taken from the SteamVR package, that was not only modified in terms of colors to resemble a human hand but also in terms of finger position so that it would sit correctly on the hand module, Figure 3.13.

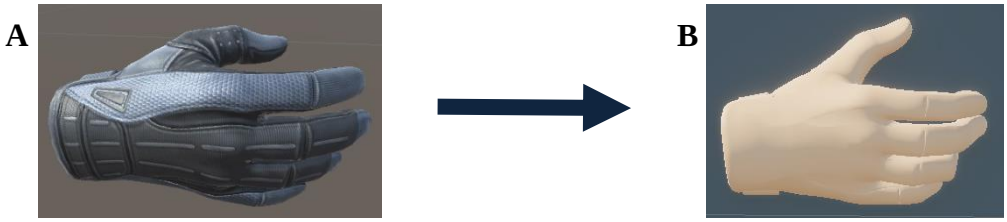

Figure 3.13 *- (A) Previous template of a glove that was (B) modified, to look like a human hand a sit correctly on the newly integrated PRIDE hand module.*

Next, it was important to animate the hand to follow the hand module's movement. Using the capabilities of Blender once again, the hand was animated. First, the armature of the hand was configured with the

assistance of the VRZone team by adding bones. This creates the capability of moving each joint of the finger individually, enabling the possibility to create a more accurate animation. Therefore, each finger was adjusted during the whole movement of the hand module, creating an animation for the hand as the hand module moved, Figure 3.14. Finally, the data recorded by the hand module's sensors were related to the animation, allowing the hand module to move to the recorded angle while doing the programmed animation.

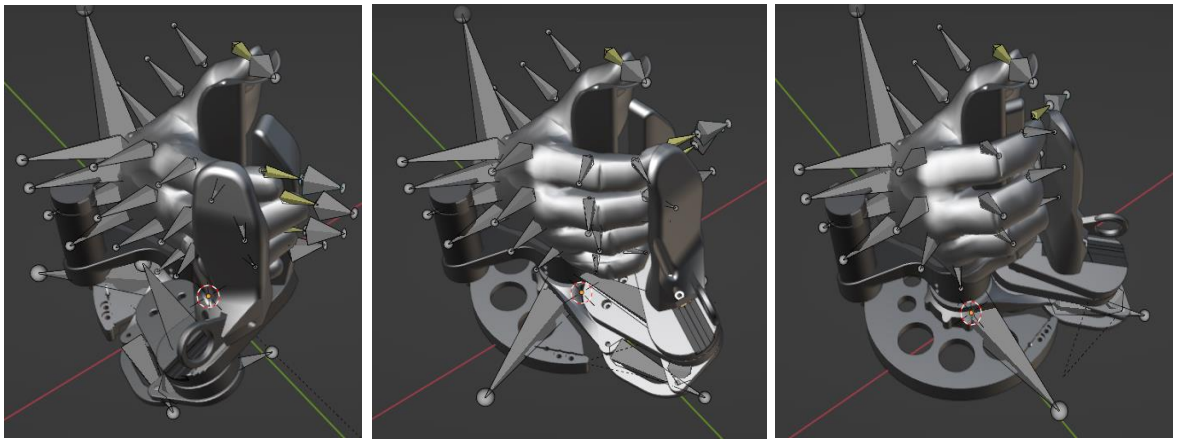

Figure 3.14 *- Configuration of the hand bones, in each finger, as well as the animation of the hand with the hand module 180º movement.*

Some scene adjustments to the lighting and shadows were also made to create more vivid colors and a more realistic experience.

3.3.1 Kinematic accuracy

In the interest of studying not only the accuracy of ARMin's digital twin but also its kinematic model via studying the EE position differences, a series of preliminary measurements were performed. The EE position difference was extracted in three different conditions: Real Robot (RR) - Digital Twin (DT), Real Robot - Forward Kinematics (FK), Digital Twin - Forward Kinematics. The data was acquired between different positions on a table and by performing some specific poses, e.g., lifting the arm and touching the shoulder. The EE position was also recorded in all measurements, both table heights and poses. These measurements will help us to determine if there is any position deviation of the digital twin relative to the virtual robot.

3.3.1.1. Experimental Protocol

Four 3.0 Vive Trackers were used to track various mechanical links to account for position differences between the VE and reality, Figure 3.15. Two trackers were placed on the height-adjustable column of the exoskeleton, able to adjust to the patient’s height, and fixed during training. Tracker B's location was considered a fixed reference, where the digital twin position would match its position. A third tracker was placed in ARMin’s column. Finally, a fourth tracker was placed in the EE position.

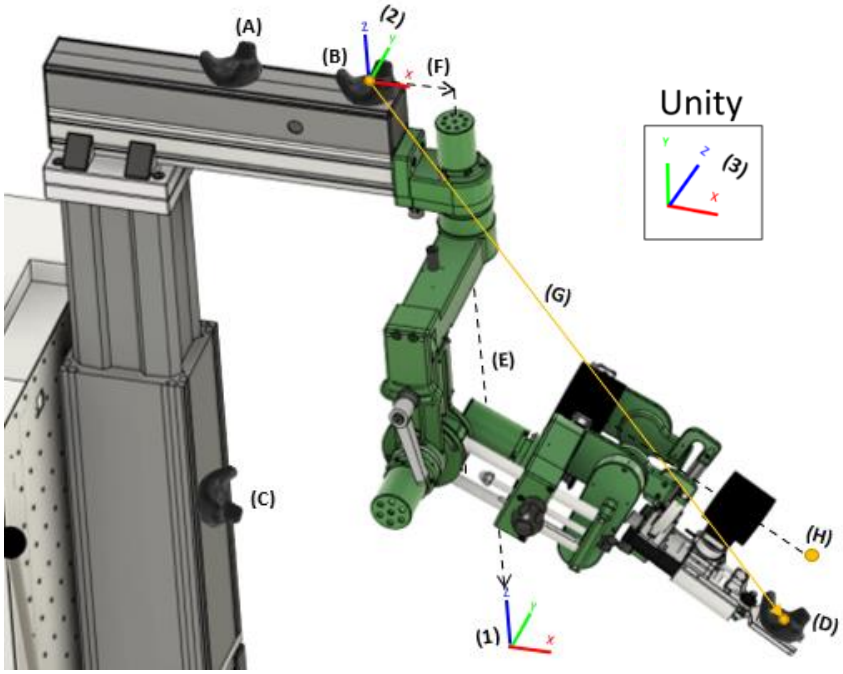

Figure 3.15 *- 4 trackers were placed (A) – (D). In the Digital Twin (DT) frame, two points were placed in approximately the same positions as trackers (B) and (D). The Real Robot (RR) frame origin was considered as the center of tracker (B), with the coordinate system (2). In the Forward Kinematics (FK) model, the origin was already set as (1) on the floor. Therefore, the positions represented in frame (1) were transformed to frame (2) with a translation along (E)+(F). In the DT, the origin was in the same position as the RR frame (2), but the axes were based on the left-hand rule, since it is Unity's default coordinate system (3). Therefore, a rotation matrix was applied so the coordinate system would match the RR frame (2). Finally, a vector was created, from the origin to the EE position (D), vector (G), for each environment.*

The position differences of the end-effector between three conditions: RR, DT, and FK. and the position coordinates were calculated individually for each. Considering the reproducibility of the acquisition, data was measured at five evenly distributed positions in a circular trajectory with a radius of 0.32 m at two different heights (Figure 3.16), with the table at 0.62 m and 0.81 m, for a total of ten positions. ARMin was kept at a static height of 1.44 m. The robot was moved until it touched the center of the cross. This procedure was repeated three times per point. A third data acquisition was made to obtain the accuracy from more diverse poses, considering that the exoskeleton robot is intended for rehabilitation. Here, six poses that a person after a stroke might perform in a rehabilitation session or during ADLs were performed (Figure 3.17): lifting the right arm, doing a handshake, touching the nose with the index finger, touching the back of the head, placing the arm across the chest, and touching the opposite shoulder. Each pose was repeated three times, and the passive joints' position and rotation did not change.

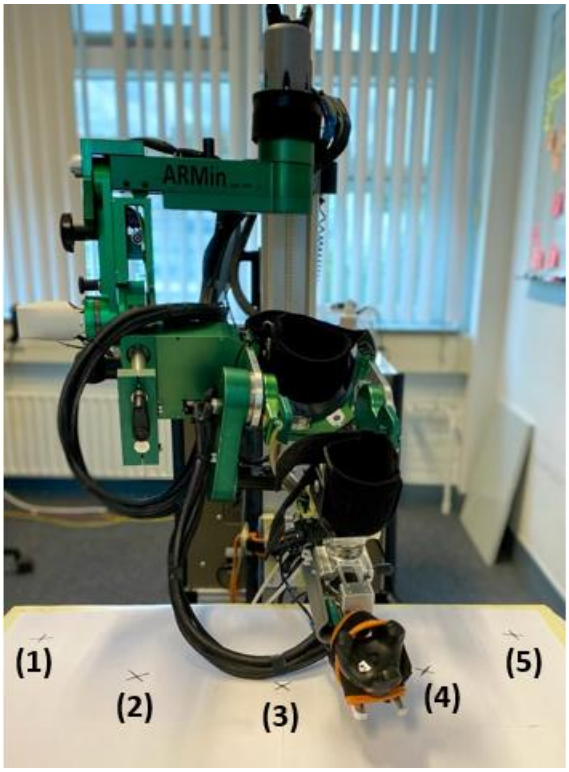

Figure 3.16 *- End-effector position difference acquired in 5 points (1)-(5), evenly distributed in a circular trajectory with a radius of 0.32 m over the table and each repeated three times. This procedure was performed with the table at a height of 0.62m and 0.81m. The robot was kept at a height of 1.44 m.*

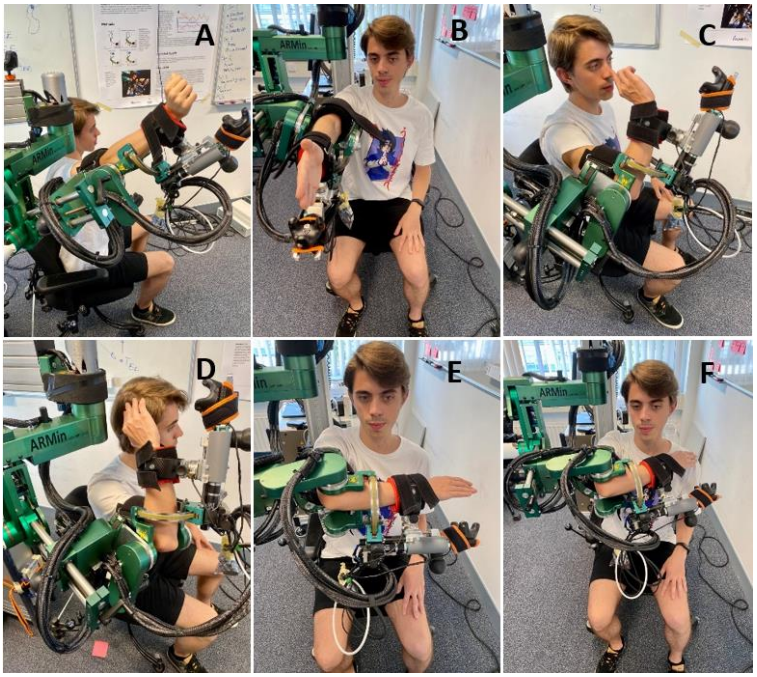

Figure 3.17*- Performed poses from which the position difference of the end-effector was obtained. These are poses that a patient might perform in ADLs or rehabilitation sessions, namely: (A) lifting the arm, (B) doing a handshake, (C) touching the nose with the index finger, (D) touching the back of the head, (E) arm across the chest, (F) tapping the opposite shoulder.*

3.3.1.2. End-Effector Position Adjustments

In line with the objective of the measurements, the vectors from the frame origin to the end-effector were calculated for different poses. However, to compare position differences, they must first be comparable, and therefore, the vectors needed to be aligned and adjusted accordingly.

For the RR coordinate frame, considered the ground truth, a plane was created using trackers (A), (B), and (C), Figure 3.15, where the x axis followed the direction of the vector $\overrightarrow{AB}$, and y was the normal vector of the plane, calculated using equation:

$$y = \overrightarrow{AB} \times \overrightarrow{AC} \quad 3.1$$

The z vector was the cross product between x and y. Then, the vector $\vec{G}$, defined as:

$$\vec{G} = \overrightarrow{BD} \quad 3.2$$

was calculated, where D is the EE tracker's center point.

In Unity's virtual environment, where the DT was located, the process was similar, where two points were placed in the same position as a tracker (B) and the end-effector position (D). Since Unity's default coordinate system uses the left-hand rule (3), the rotation matrix R:

$$R = \begin{pmatrix} 0 & 0 & 1 \\ -1 & 0 & 0 \\ 0 & 1 & 0 \end{pmatrix} \quad 3.3$$

was applied so that the axes would be the same as the RR coordinate frame.

With the FK model, it is possible to immediately know the position of the end effector. However, the origin of this frame (1) was different from the RR origin. Taking this into account, the positions were transformed to frame (2) with a translation along $\vec{E} + \vec{F}$ where $\vec{E}$ corresponds to the height of ARMin of 1.464 m and $\vec{F}$ a translation on the $x\ axis$ of 0.13 m, so that:

$$\vec{E} + \vec{F} = (0.13, 0, -1.464) \quad 3.4$$

Another important consideration was that, in the model, the end-effector is defined to be on the height of axis 5 (forearm pro/supination). Thus, the tracker is lower. By assuming the center point of the tracker as its origin, at the height of 0.025 m, and considering that the end effector position in FK (H) was 0.114 m above the tracker's position (D), the tracker was at a distance:

$$x = (0.114 - 0.025) \quad 3.5$$

from the end-effector. By also accounting for the orientation of the EE, the final vector (G) for this model was as follows:

$${}_1\overrightarrow{V_{BD}} = {}_1\overrightarrow{V_{EE}} + \vec{E} + \vec{F} + \overrightarrow{V_{HD}} \quad 3.6$$

Where ${}_1\overrightarrow{V_{BD}}$ is the vector, from point (B) to (D), for the FK frame that has (1) as its origin (Figure 3.15), ${}_1\overrightarrow{V_{EE}}$ is the vector from the FK model origin (1) to the EE position in the model (H), and $\overrightarrow{V_{HD}}$ is the vector from point (H) to point (D). The final step was to compare the three calculated vectors, now all within the same frame, with each other to get the distance difference between them.

3.3.2. VR Game Prototype

To test the digital twin, a prototype game was developed in virtual reality. This game consists of the user

building a pyramid made of six cubes in the shortest time possible. Thus, in front of the user was a table and six cubes positioned in different places to force the user to move to different positions, Figure 3.18. Additionally, there were three targets in the center of the table. The table was an existing model taken from the Unity Asset Store.
When grabbing a cube with the virtual hand module, the user would have to place this cube in one of the targets and would not be able to drop the cube or grab another one before doing so. This was achieved by adding a box collider to the hand module and the cube and a spherical collider to the targets. In the process of grabbing a cube with the digital twin, when the hand module collider touched the cube collider, a script would be triggered to move the cube to the center of that handle, seeming as if the user grabbed it. This center point was created as a GameObject to facilitate the procedure. To prevent other components from interacting with the cubes' colliders, the script would first check if the collider touching the cube was the hand module one. Also, to distinguish whether the user's hand was opening or closing, and therefore whether the user was trying to grab the cube, it was only possible to grab it under two other conditions. First, the hand module animation value, which ranged from 0 (hand fully opened) to 1 (hand fully closed), was recorded in every frame. If the new value was bigger than the previous one, then it meant the user was performing a grasping motion. Second, it was established that this value had to be between 0.27 and 0.40 since these would be the values for which the hand would have enough opening to grasp the cube.

Upon placing the cube on the desired target, a script would be triggered when the hand module collider touched the target collider, and the cube's position would be changed to the center of that target. To facilitate the cubes' placement, as seen in Figure 3.19, the target colliders were bigger than the GameObject. Additionally, when the two colliders touched, the cube would automatically move to the middle of the desired target location, as if it had a magnet. To prevent more than one cube from being placed on a target, the target's collider was disabled once it had a cube on it.

When two adjacent cubes had been placed, a cloned target would appear on top between them to continue the pyramid's construction. Thanks to the *Instantiate* function, this new target would pop up at the designated coordinates (x', y', z'), where:

$$x' = (x_{target1} + x_{target2})/2 \tag{3.7}$$

$$y' = \left|y_{cube\_in\_target1} - y_{target1}\right| * 2 + y_{target1} + 0.003 \tag{3.8}$$

$$z' = z_{target1} \tag{3.9}$$

The 0.003 was an arbitrary value, so the new target clone was not exactly at the y of the top face of the placed cubes, as some display errors were noticed when this happened. It is also important to note that the coordinates of the targets, in Unity, are the coordinates of the center point and that:

$$y_{target1} = y_{target2} \tag{3.10}$$

$$z_{target1} = z_{target2} \tag{3.11}$$

and therefore, it can be used either of them. A flow chart of how the game works can be found in Figure 3.20.
When the user finishes building the pyramid, a text will appear on the screen congratulating them and showing how long it took to complete the task in minutes and seconds.

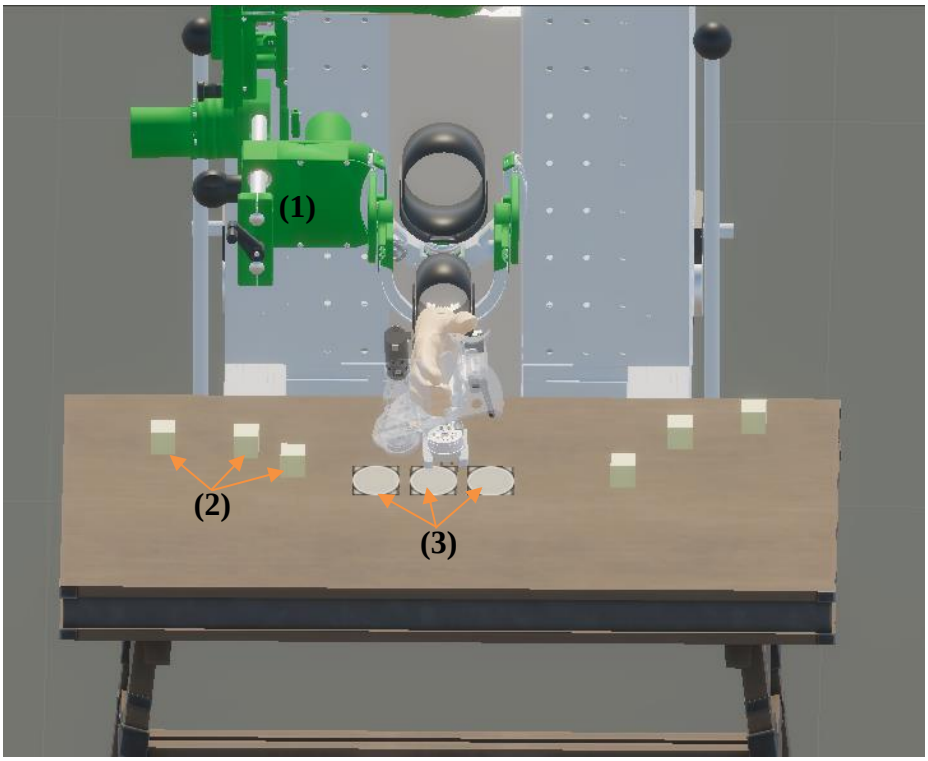

Figure 3.18 *- VR Game Prototype Components: (1) Digital twin of the ARMin upper limb rehabilitation exoskeleton robot, (2) cubes that the user needed to grab with the virtual hand module to build a pyramid, (3) targets were the cubes needed to be placed. Both the cubes and targets were placed on a table.*

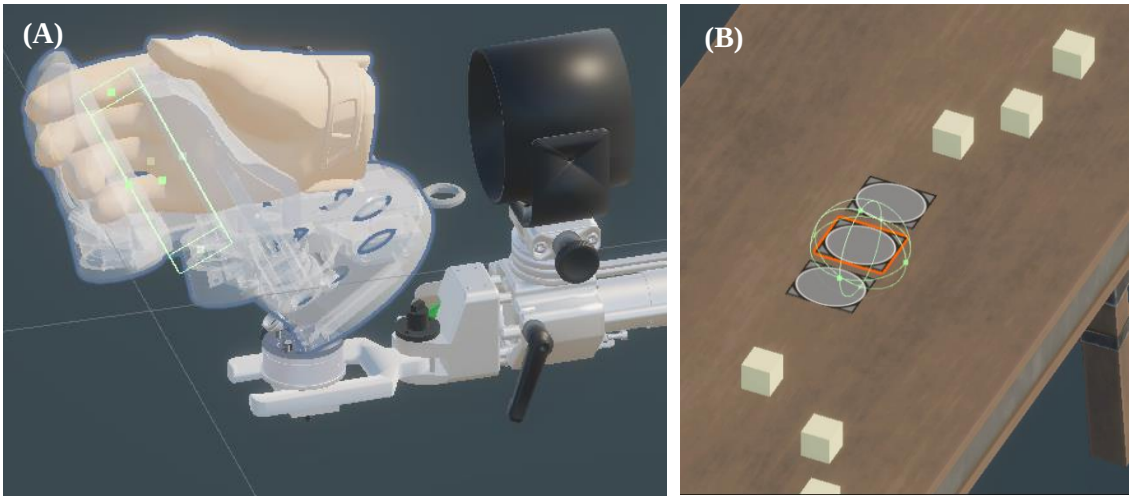

Figure 3.19 *- (A) Hand module box collider and (B) target's spherical collider. Both colliders were used to grab the cubes and place them in the desired location, respectively.*

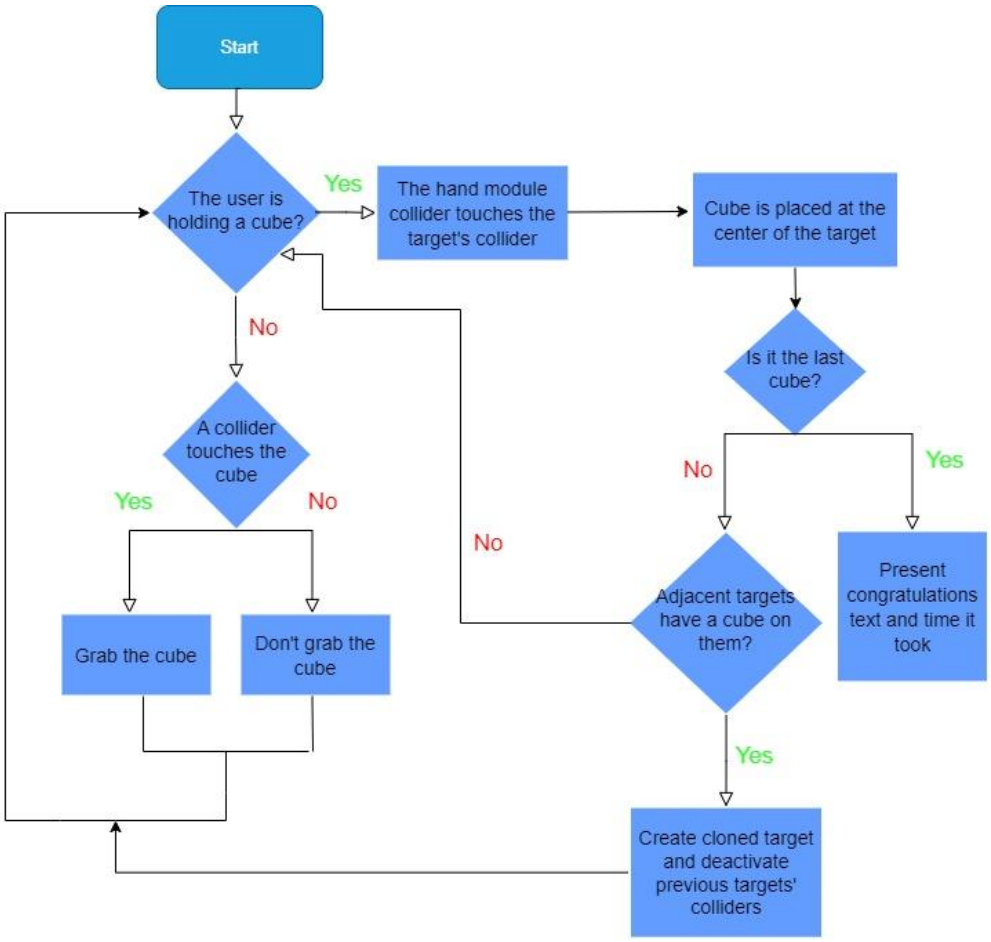

Figure 3.20- *Schematic visualization of how the developed game in VR behaves.*

4. Results

This chapter aims to illustrate the most important findings of this study. First, the results concerning assembling the PRIDE hand module in the ARMin rehabilitation exoskeleton robot and the parts designed and fabricated for that integration are presented. Next, the developed ARMin visualization model is shown, as well as a prototype VR game that was developed to test this model. Finally, the data regarding the preliminary study of the kinematic accuracy of the digital twin and the exoskeleton kinematic model are presented.

4.1. Hand Module

After several iterations and taking into account the requirements presented in the methods, all the most relevant prototypes until the final version of the top part (part 1) are presented in Figure 4.1
The final part can be divided into two parts: a circular piece in direct contact with the force/torque sensor and a rod. The rod is designed to sit firmly inside the hand module and with a 25° tilt to counterbalance its angle. Once the rod comes out of the PRIDE hand module, it becomes vertical so that the circular piece where the rod ended is parallel to the sensor. Two 2mm screw holes were added at the top of this rod, adding an attachment point to the hand module. The height of the rod and the circular part were adjusted, allowing the hand to be in the natural resting position and not preventing the hand module from performing its full range of motion. These adjustments were considered when designing the other parts that would help in the integration of the hand module. Some fillets were also added, especially to the base of the rod to reduce tension and possible breakage at these points.
Due to the new EE of the hand module being 6 cm forward from the former one, and after several iterations, a balance was arranged in terms of how far back the rod reaches, while remaining within the limits of the circular part. Staying within those limits provides a greater ability to hold the weight of the hand module. Finally, some fillets were added, and cuts were made in the back of the rod to make it easier to screw in the rear screws.

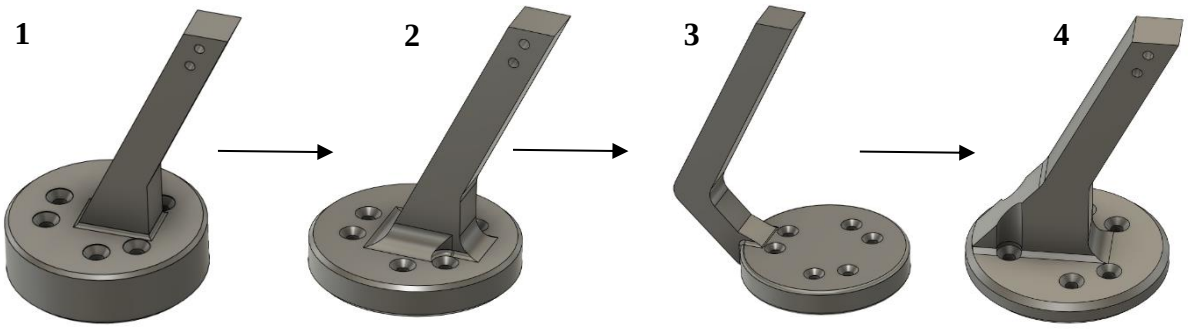

Figure 4.1 *- The three prototypes of the top part that makes the connection between the new hand module and the force/torque sensor (1-3) and the final version of this part (4).*

Since the next part needed would connect directly with the force/torque sensor from below, it made sense to give it the same circular shape as the sensor and with matching screw holes. As stated previously, the

height of this second piece that connected the force/torque sensor to ARMin was influenced by the top part's height, designed so that the hand would be on the same axis as the arm. Finally, two 4mm screw holes were added to fix this part and the two below it to the extremity of ARMin. This decision was made considering that it would not be possible to use an 8mm screw and pin as before since the screw was too wide and long, and there was not enough room for the screw and pin to remain inside the parts.

Finally, the following two parts were adjusted to fit in the extremity of ARMin as previously, while also enabling the adjustment of the distance from the forearm to the fingertips. The holes were also changed to two 4 mm holes, and in the last one, a chamfer was added to reduce the probability of bending or breaking. The result of all the parts, as 3D models, as well as the new hand module mounted, can be seen in Figure 4.2.

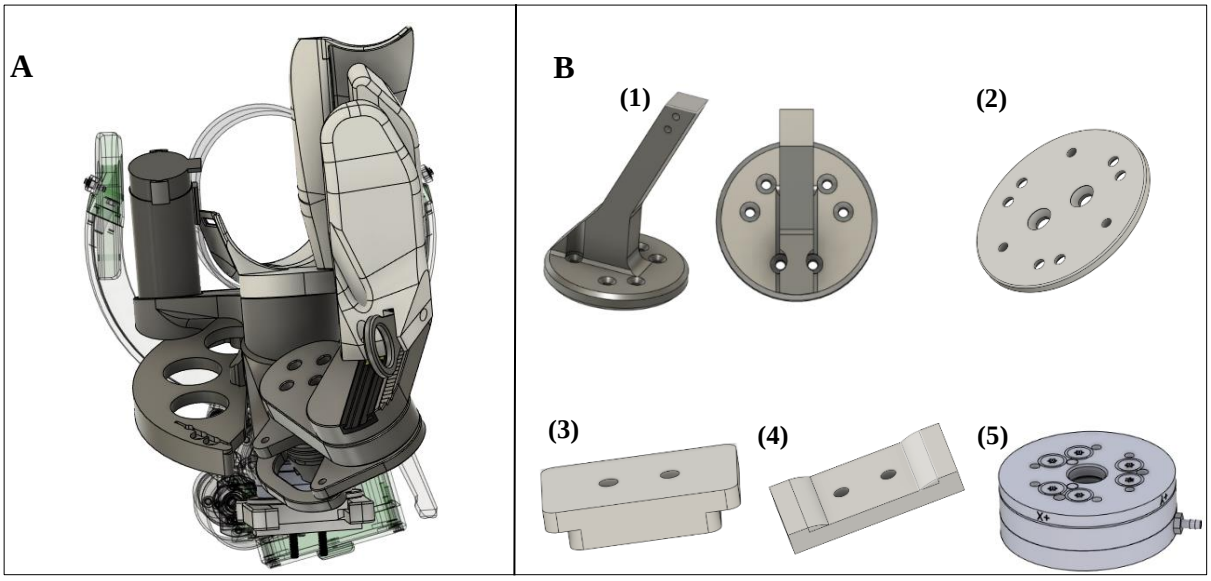

Figure 4.2 *- (A) PRIDE hand module attached to the ARMin exoskeleton and (B) parts to make that attachment possible: (1) top part that makes the connection between the hand module and the force/torque sensor; (3) part that connects to the force/torque sensor from below and to ARMin's extremity; (4)-(5) parts that slide across the extremity, making it possible to adjust the distance from the forearm to the fingertips; (5) FTD-Mini-45 SI-580-20 force/torque sensor.*

4.2. ARMin Visualization

ARMin's digital twin model, with seven active and three passive joints, is represented in Figure 4.3. Therefore, every joint was implemented. The colors of the components were also respected, being similar to those of the real robot. One more DoF was added with the implementation of the hand module, both in the exoskeleton robot and the virtual model.

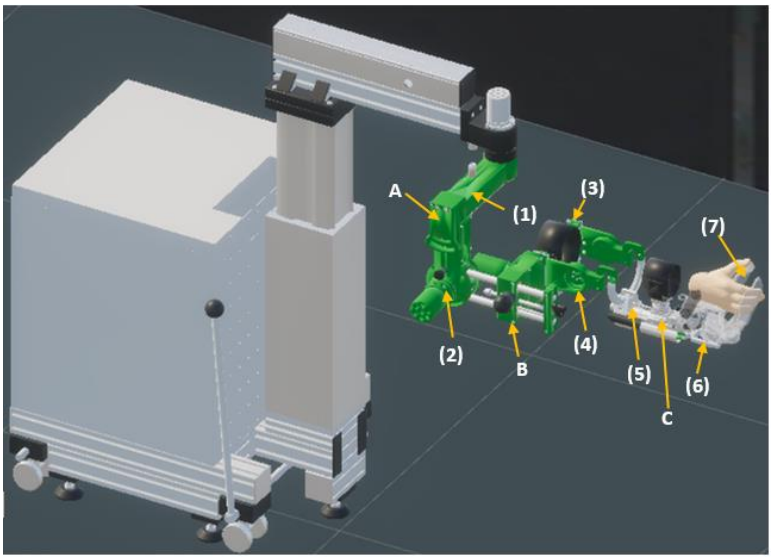

Figure 4.3 *- Digital twin of ARMin, in Unity's virtual environment with 7 Active Joints (1)-(7) and 3 Passive Joints (A-C).*

In Figures 4.4 a) and 4.4 b) it is possible to see a user interacting with the exoskeleton as well as the VE. The user would sit on the chair comfortably to use the robot and be equipped with an HMD to see and interact with the virtual environment while the base stations mounted on the wall captured the user's position. Consequently, what the user sees, and his field of view is also represented, with both images corresponding to the same moment in time.

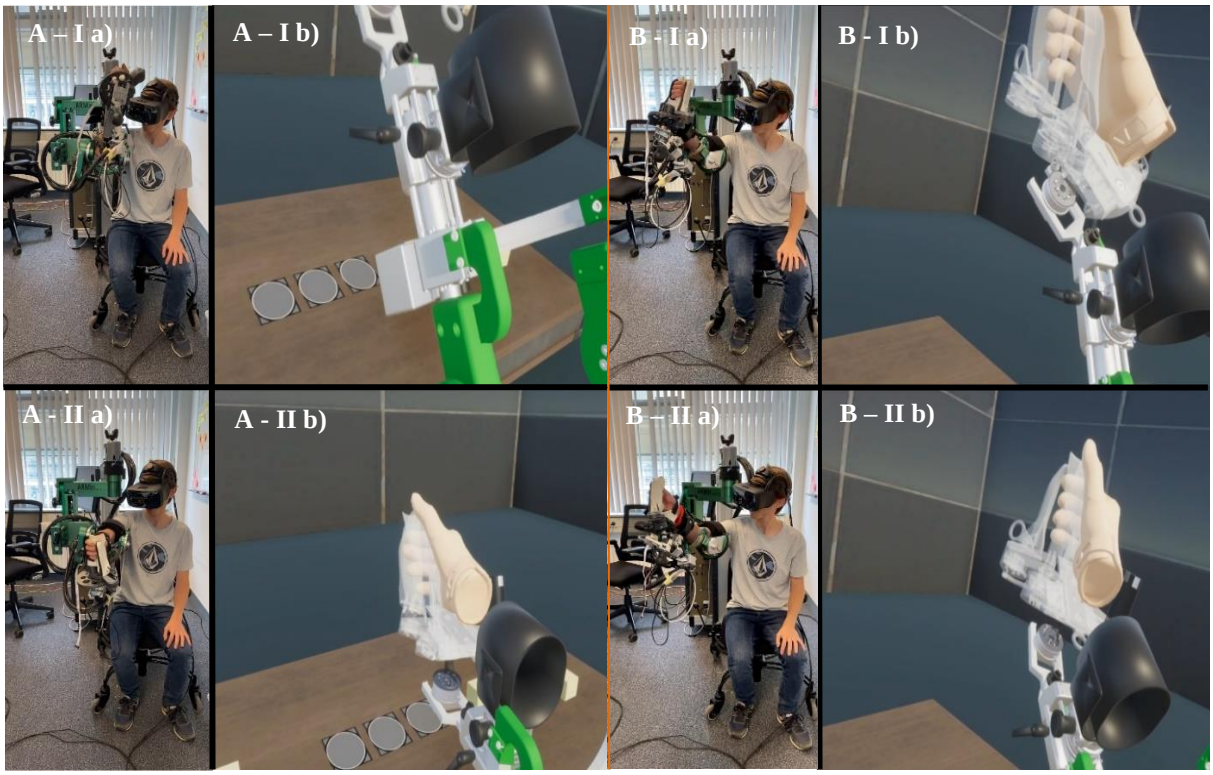

Figure 4.4 a) *- User experiencing VE while controlling the digital twin with the ARMin upper limb rehabilitation robot. The user is performing different poses and movements, and it is possible to see what the user is visualizing, via the HMD, at that exact moment, in the image to the right of each one: (A-I) and (A-II) – lowering/lifting the shoulder; (B-I) and (B-II) – moving the wrist.*

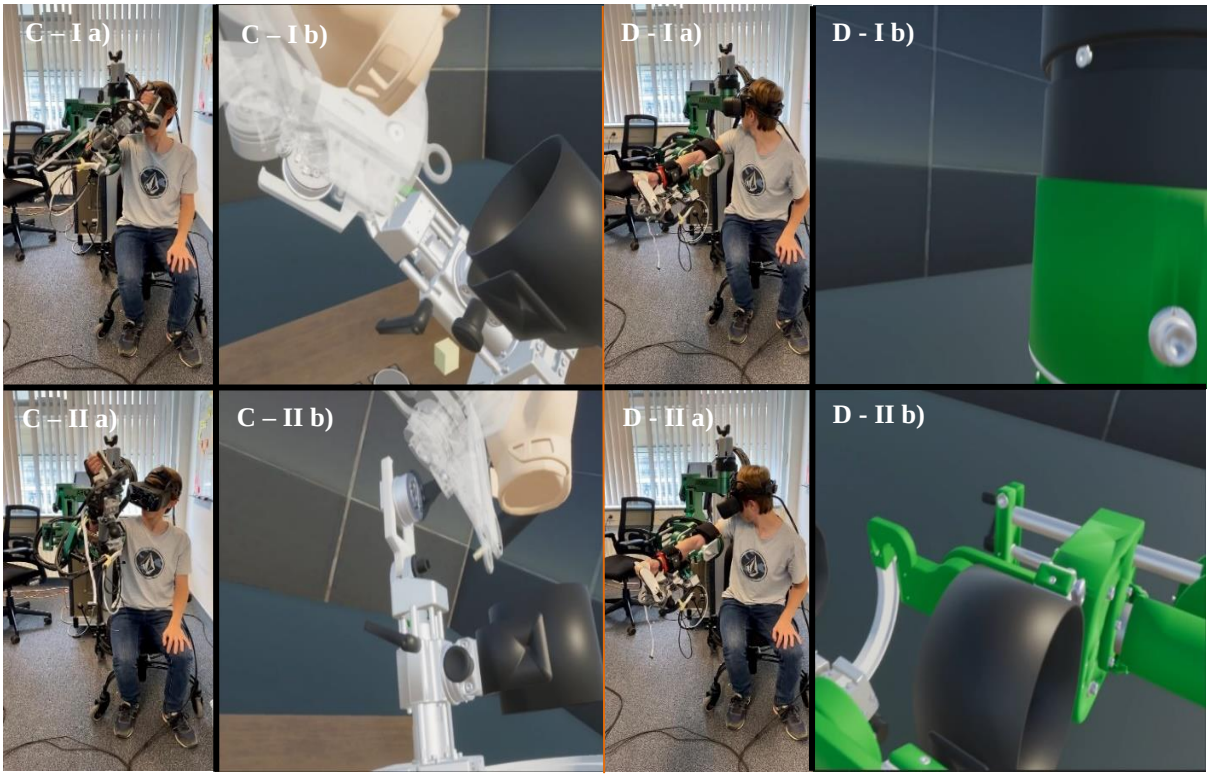

Figure 4.4 b) *- User experiencing VE while controlling the digital twin with the ARMin upper limb rehabilitation robot. The user is performing different poses and movements, and it is possible to see what the user is visualizing, via the HMD, at that exact moment, in the image to the right of each one: (C-I) and (C-II) – rotation of the arm; (D-I) – visualization of joint 1 and perspective on how close the robot is to the user; (D-II) – visualization of joints 3-5.*

4.2.1. Kinematic accuracy

The outcomes for all acquisitions are illustrated in Figure 4.5. In Table 4.1 it is also possible to see more in-depth the values of the mean and standard deviation for the table and poses measurements. In addition, Table 4.2 and Table 4.3 represent the average position (x,y,z) for the table and poses measurements, respectively. Lower distance values were recorded when comparing RR with DT, specifically in the lower and higher table measurements, with a mean of 0.024±0.003 m (mean ± standard deviation) and 0.032±0.003 m, respectively. A difference was registered when performing the poses (0.049±0.017 m). However, this was the lowest average value registered for the poses' measurements between different comparisons. When the three measurements were grouped, the position differences when comparing RR with DT were also the lowest, with an average of 0.036± 0.015 m.

The recordings, when comparing RR with FK, averaged 0.036±0.003 m with the lower table setting and 0.062±0.009 m with the higher table. A similar mean of 0.064±0.025 m was recorded when performing poses, but with greater variability. The combination of the measurements averaged 0.055±0.020 m.

The FK-DT relationship recorded a higher value (0.059±0.001m) for the lower table measurements and an average of 0.057±0.003 m for the higher table. The pose data averaged 0.071±0.031m, with very high variability. Finally, the total value of all measurements was 0.063±0.020 m.

Overall, the data regarding the poses have more variability. This adds up when we add the pose values with the lower and higher table values, creating a more considerable interval in the boxplot and more outliers, especially in the FK-DT comparison. The values with the shoulder tap and the arm across the chest show a larger difference between measured distances between comparisons (Figure 4.6). On the other hand, touching the nose and back of the head registered the lowest distances overall. Regarding the vector coordinates, the recorded y values did not change much between different calculations and comparisons, contrary to the z-axis that recorded the most different values. This is the case for every data acquisition method.

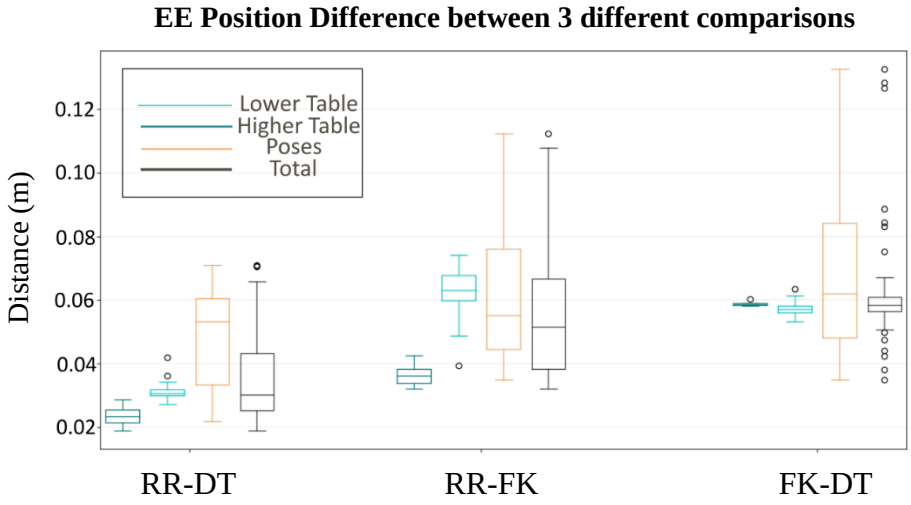

Figure 4.5 *- Distribution of distance values calculated in the three data acquisitions - Lower Table (green); Higher Table (blue); Poses (orange) - and the combination of these 3 (Total, in black), when comparing Real Robot (RR)-Digital Twin (DT), Real Robot (RR)-Forward Kinematics (FK) and Forward Kinematics (FK)-Digital Twin (DT).*

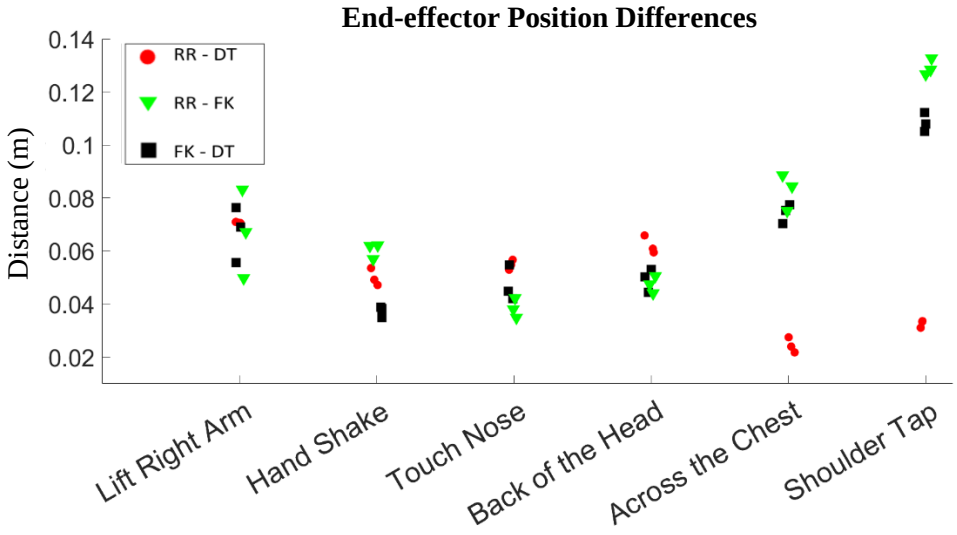

Figure 4.6 *- Distance values for each pose (m). The poses were performed 3 times, calculating the distance between end effectors in Reality-Visualization (red circles), Reality-Simulink (black squares) and Simulink-Visualization (green triangles).*

***Table 4.1**- Mean and standard deviation values for the Real Robot (RR) - Digital Twin (DT), Real Robot (RR) - Forward Kinematics (FK) and Forward Kinematics (FK) - Digital Twin (DT) comparisons and respective measurements with the lower table, higher table, and the performed poses.*

Comparison	Measurements	Mean	Standard Deviation
RR- DT	Lower Table	0.024	0.003
	Higher Table	0.032	0.003
	Poses	0.049	0.017
	Total	0.036	0.015
RR - FK	Lower Table	0.036	0.003
	Higher Table	0.062	0.009
	Poses	0.064	0.025
	Total	0.055	0.020
FK - DT	Lower Table	0.059	0..001
	Higher Table	0.057	0.003
	Poses	0.071	0.031
	Total	0.063	0.020

***Table 4.2** - Average position (x, y, z) measured with a table at 0.62 m and 0.81 m, through Real Robot, Digital Twin, and the Forward Kinematics model.*

Measurements	Points/Position	Real Robot	Digital Twin	Forward Kinematics
Lower Table	1	(0.526, -0.398, -0,786)	(0.535, -0.400, -0.767)	(0.503, -0.382, -0.812)
	2	(0.647, -0.219, -0.784)	(0.657, -0.219, -0.765)	(0.623, -0.206, -0.811
	3	(0.691, 0.003, -0.784)	(0.702, 0.005, -0.763)	(0.666, 0.001, -0.809
	4	(0.642, 0.226, -0.786)	(0.653, 0.232, -0.763)	(0.623, 0.210, -0.808
	5	(0.528, 0.391, -0.788)	(0.538, 0.400, -0.764)	(0.521, 0.366, -0.809)
Higher Table	1	(0.675, -0.362, -0.587)	(0.652, -0.352, -0.572)	(0.631, -0.352, -0.622)
	2	(0.758, -0.187, -0.583)	(0.735, -0.182, -0.562)	(0.713, -0.192, -0.615)
	3	(0.789, 0.012, -0.573)	(0.762, 0.011, -0.561)	(0.745, -0.004, -0.614)
	4	(0.754, 0.213, -0.570)	(0.729, 0.201, -0.563)	(0.717, 0.179, -0.615)
	5	(0.665, 0.384, -0.576)	(0.644, 0.365, -0.566)	(0.641, 0.339, -0.616)

***Table 4.3** - The average position (x, y, z) measured by performing specific poses through the Real Robot, the Digital Twin, and the Forward Kinematics model.*

Vector (x,y,z)/Poses	Real Robot	Digital Twin	Forward Kinematics
Lift right arm	(0.456,-0.403,-0.051)	(0.434, -0.341, -0.076)	(0.406, -0.398, -0.093)
Handshake	(0.774, -0.104, -0.457)	(0.754, -0.063, -0.438)	(0.744, -0.105, -0.478)
Touch nose	(0.567, 0.044, -0.187)	(0.521, 0.073, -0.196)	(0.540, 0.055, -0.220)
Back of the Head	(0.400,0.032, -0.121)	(0.360, 0.062, -0.157)	(0.368, 0.016, -0.155)
Across Chest	(0.497, 0.254, -0.544)	(0.483, 0.264, -0.561)	(0.464, 0.276, -0.481)
Shoulder Tap	(0.394, 0.312, -0.504)	(0.377, 0.314, -0.532)	(0.347, 0.313, -0.407)

4.2.2. VR Game Prototype

The developed VR game is presented in Figure 4.7. It is possible to see the user controlling the digital twin while grabbing a cube with the implemented virtual PRIDE hand module and finishing building a pyramid (Figure 4.7 (A)). Further, the mechanics of how the pyramid is constructed and how the targets are presented gradually can also be analyzed (Figure 4.7 (B)). A new target appears when two adjacent targets have a cube

on them. However, if two adjacent targets do not have a cube, the next target does not present itself.

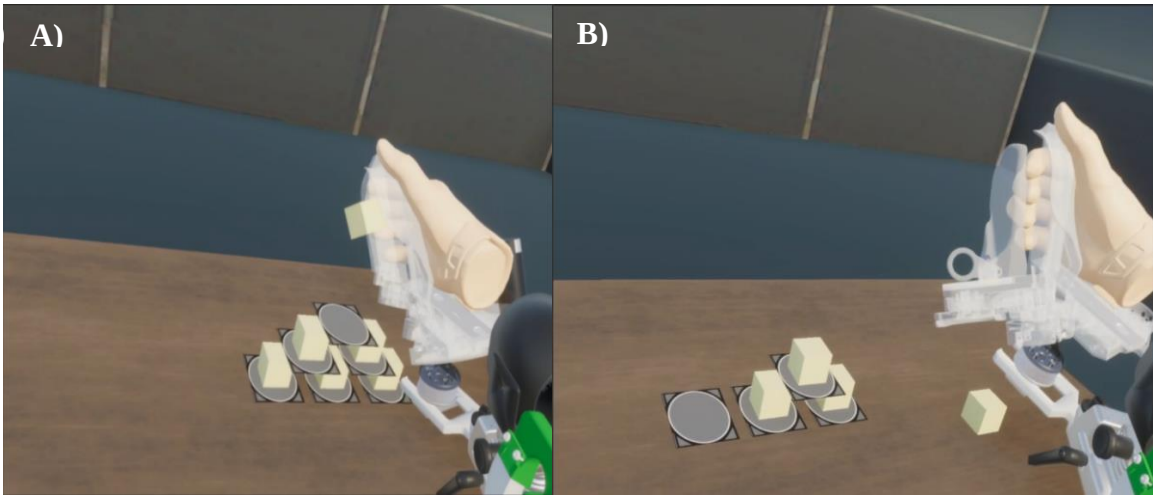

Figure 4.7 *- (A) User building a pyramid by grabbing the cubes with the digital twin's PRIDE hand module and placing them in the desired target. (B) If two adjacent targets have a cube, a cloned target appears to continue the pyramid construction however, if this does not apply, the next target does not present itself.*

In Figure 4.8, the on-screen text congratulating the user and showing how long it took to complete the task, in minutes and seconds, Figure 4.8 (A), and the end-screen thanking the user for participating, Figure 4.8 (B), are presented.

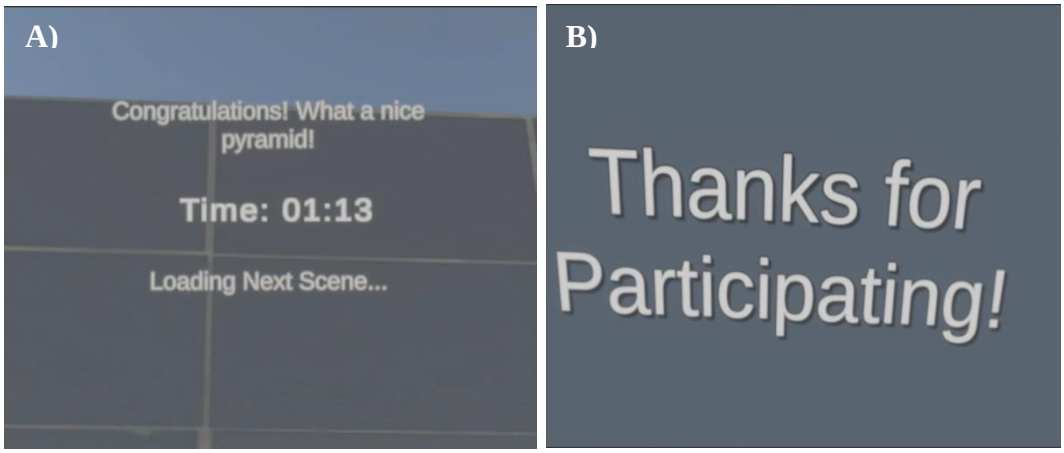

Figure 4.8 *- What the user sees after completing the pyramid. (A) First, a text congratulating him and presenting the time it took to finish the building process, and (B) then the displayed text thanking for the participation.*

5. Discussion

This chapter provides an overview of the presented work and results while illustrating potential improvements. Firstly, the hand module integration and the parts designed and developed are discussed. Then a discussion about the visualization model is given with ARMin's digital twin. This section also contains two brief analyses of the developed VR game prototype and the evaluation of the exoskeleton's kinematic model and the digital twin's kinematic accuracy.

5.1. Implementation of the Hand Module

In the first part of the analysis (Section 4.1), different prototypes were designed and fabricated for all four parts that enabled the PRIDE hand module to be integrated into the ARMin upper limb rehabilitation robot until they satisfied the requirements presented in Section 3.1. The result for the four parts and the new hand module integrated in ARMin can be seen in Figure 4.2. The hand module was positioned at the same height as the forearm, avoiding discomfort for the user while ensuring that the user's hand remained in a neutral position and was able to perform the 180° movement without any obstruction. The first part was the one that received the most iterations, as seen in Figure 4.1, due to being the one with more constraints and requirements and due to the complexity of the new hand module compared to the previous EE.

By integrating a hand module, the ARMin exoskeleton gained another degree of freedom, allowing a 180-degree range of finger movement. In addition, the user now has hand and wrist support, allowing the hand to be positioned more comfortably. Many ADLs rely on grasping and reaching movements as stated in the questionnaires done by *Rätz et al.* [1]. Consequently, grip training is vital. As a result, this integration might enable future rehabilitation exercises focused on improving the quality of life of people after a stroke.

However, the integrated parts and the hand module have some limitations. First, most of the components that make up PRIDE are 3D printed, as well as the parts fabricated and used to mount this in the exoskeleton. Although it allows for rapid prototyping, this characteristic limit the rigidity of those parts according to the material used for the printing, which reduces their durability.

Regarding the PRIDE hand module design, it was noted during the integration and testing that the hand and wrist support was uncomfortable when rotating the wrist. This may prevent the user from performing the movements to their full extent. Due to limited time, designing and manufacturing a solution to this problem was not possible, but it should be noted for future use.

Another important factor is the arm, especially the length of the forearm Nonetheless, with the shown implementation method, it was possible to incorporate this device with the correct height despite all limitations while reducing the grasping position difference from 6 cm to 3 cm. However, this position offset is still noticeable, making it difficult for some users to extend their fingertips fully. Since this limitation reduces the population that can use the device to its full extent, it is important to improve this further by reducing the remaining 3 cm offset.

5.2. Visualization

For the second part of this work, a digital twin of ARMin was successfully developed and implemented using software such as Unity and Blender, along with virtual reality through the use of SteamVR and equipment such as base stations, trackers, and the Varjo-XR3 head-mounted display. Section 4.2 represents the digital twin model (Figure 4.3) with the seven active DoF and three manually adjusted joints. Every joint was fully implemented and connected, creating a copy of the real exoskeleton. Furthermore, the connection with the actual robot worked as intended, enabling the digital joints to move along with the real ones. By analyzing Figures 4.4 a) and 4.4 b), it can be seen that the digital twin is performing the same movement as the user. The user's field of view comprises the fifth joint to the end of the hand module, which is similar to the real world. The added hand visualization, previously modified from the SteamVR glove template, resembles a human hand and appears to be in the correct position, being rested on the handle of the hand module and with each finger positioned as intended. Also, thanks to the transparency added to the PRIDE hand module, the user can see past it, which does not block their vision and makes it easier to perform tasks.

VR opened the possibility of creating a more realistic experience and environment. Despite some difficulties due to using the Varjo XR-3, a recent headset, and with some incompatibilities and lack of optimization when working with other equipment, such as trackers, the implementation was successful. The chosen HMD allowed the creation of a high-definition environment and ARMin model together with the HDRP textures. One thing that should be noted is that the textures and the headset required high computing power to work and be processed well. Although the computer used met the requirements, it only met the minimums. Thus, there were some drops in performance and frames while running the VR scenario, especially in the first few seconds after running it, since the computer needed to load a larger number of elements quickly. This could possibly reduce immersion as well as increase the chances of motion sickness. To avoid these problems, it is essential to improve the computational capacity of the computer.

The hand module was integrated into the VE by developing a script to receive the data from its motor and thus perform the animation in parity with reality. However, due to the limited time, it was not possible to connect the motor of the hand module to ARMin and thus verify the hand movement according to the user's real movement. Nevertheless, a sinusoidal function was implemented to control the animation, allowing the hand module to open and close continuously. For future work, this connection must be made, not only to complete the digital twin of the robot, where all the joints move according to the real robot but also to test the developed code and whether it is correct. Further, it would be interesting to implement not only the hand but the entire arm of the patient or even an avatar. Although implementing these models would be time-consuming, it could create an even more immersive experience.

Another feature that was not given much attention due to time constraints was the settings of textures, colors, and light of the VE. By changing and studying these settings, it is possible to create a more realistic scenery and a digital twin that more closely resembles the real exoskeleton.

Although this did not register as a significant or notable problem when testing the simulation, to also improve the user experience, at least two trackers should be used instead of one, as this also allows the orientation of the ARMin to be taken into account and not just the location in the room when adjusting the digital twin position to the match the exoskeleton. Further, the position of the base stations should be optimized to avoid drift. In the case of trackers, this is seen through the drifting of the trackers' position due

to the inability of the base stations to locate them.

The developed visualization enables the possibility of studying not only the influence of this digital twin on motor learning but also the user behavior for different properties of the digital twin. This will allow for a better understanding of what positively or negatively affects the user during rehabilitation exercises, enabling not only to make the interventions more objective but also enabling to plan the tasks in a way that enhances the patient's motor recovery, increasing the quality of rehabilitation.

5.2.1. Kinematic Accuracy

In Section 4.2.1, the accuracy of ARMin's digital twin and its kinematic model via EE position differences was analyzed. The lowest end effector position differences, on average, were in the RR-DT comparison. This is a good sign since we consider the RR data to be the ground truth, which means that the visualization has good accuracy. Still, some errors are noticeable in RR-DT, as well as RR-FK. One possible explanation is that the calibration of the ARMin joints was not performed 100% correctly on all joints, causing a discrepancy between the actual position and rotation and the value transmitted by the FK model, which then causes a more significant error compared to reality.

FK-DT has the most considerable data variability and overall higher EE position differences. Since the values from the FK model for each joint are directly used to move the digital twin joints, this is surprising. In terms of the ARMin digital twin joints, they were programmed to compare the previous value with the new value they got from the robot. If this value differed from the previous one, they would shift this difference to the desired orientation. However, since this comparison was made on each frame, this can add minor errors that increase with time, especially considering the possibility that, for example, a position was not captured during one or more frames. Therefore, for future use and to minimize such errors, it is suggested to directly set the target rotation, known through the FK model, instead of incrementally changing it based on the difference from the previous state. This influences not only the table measurements but also the poses.

The table measurements had lower variably when compared with the poses, where the lower table variability was lower than the higher setting. Since the only difference between them is the height, which is affected mainly by the arm elevation and shoulder flexion/extension joints, it is possible that the implementation of these joints in Unity is not truly accurate.
Regarding the poses, there is, in fact, a big data variability that was less present than in the table measurements. Despite the passive joints being in a constant position, it is tough for the user to perform the poses in the same way they did previously. At first glance, this should not interfere with the distance difference but can add up errors if, as stated previously, there are differences in the FK or DT model.

When examining each position in more detail, it becomes clear that there is little variation in the values between comparisons. Nevertheless, in the movements of putting the arm across the chest and tapping the shoulder, there is an apparent disparity between the distance difference in the DT-RR in comparison with the other two. From the joint data and analyzing these two movements, we can see that the one thing in common in both is the elbow rotation to an angle of approximately 90º. Since the joint data is retrieved from the FK model, and these differences consider the FK values, the errors may remain in the VE. The elbow joint was the most difficult one to implement due to the robot's tilted fit, which is not easy to copy in the

virtual environment developed in Unity. Therefore, it is possible that the position and movement of this joint are not 100% accurate, which causes this discrepancy.

One more thing to consider is that the tracker's position is not constant and depends on how well the lighthouse sensors capture their position. It is possible that, in some measurements, especially in specific movements/poses, they could not capture their actual position because ARMin blocked their view. This can cause a larger recorded distance value compared to reality.

The y position values are all very similar between the three different calculations. This was already expected since we did not have to adjust the y-axis in FK-RR, and it only rotated in the DT-RR frame, unlike the other axes.

There are some differences registered on the x-axis, but the z-axis is the one in which the differences in values are more noticeable. One important thing to notice is that the (E) and (F) values were measured with a tape measure, leading to measurement errors in the millimeter range. Additionally, due to the lack of documentation stating the tracker's origin, it was assumed to be at the center of the main body. However, if this is not the case, it creates a height difference and error of ±0.025 m in the z-direction.

With these results, we hypothesize that for low values in the centimeter range, users should not experience any problems with immersion or embodiment.

5.2.2. VR Game Prototype

In section 3.3.2, a prototype of a VR game was developed. Due to time constraints and the impossibility of connecting the hand module to ARMin, as discussed above, the game could not be tested with participants. Thus, it could have been optimized in terms of code and bugs. Nevertheless, the basic principle and mechanics were achieved, as it is possible to move the digital twin to grab and drop cubes on targets. The last cube triggers a congratulations screen that displays the time it took to complete the task. Reducing the opacity of the hand module allowed the grasped cubes to be viewed more easily, creating the chance to make it easier to grasp and place the cubes on the targets and, thus, build the pyramid.

Still, it would also be important for this game, besides the proper connection of the PRIDE and adjustment of the animation, to test it and receive feedback from the participants, both stroke patients, and physiotherapists, to improve it according to the patient's future needs. One feature that could be added in the future is tactile feedback, as the PRIDE hand module has haptic rendering capabilities, simulating grasping sensations and therefore creating a more immersive experience. It would also be interesting for the VE to communicate with the robot, giving feedback to the person. An example of this would be the digital twin not being able to pass through the table when coming into contact with it. This way, when the digital twin collides with the table, information would be sent to the robot to offer resistance that would prevent the person from lowering his arm any further. This would not only make the experience more immersive but would also require the user to perform more complex movements to grab the cubes.

Finally, it should be noted that this technology's future patients and users will be mostly older adults. As they use technology, older adults experience a variety of physical or cognitive hurdles, such as impaired

cognition and difficulty hearing or seeing. Aside from these physical restrictions, the elderly also encounter obstacles like lack of familiarity and access, discomfort when seeking help, trust challenges, and privacy concerns [107]. This may impose difficulty in adaptation and use. Therefore, it is crucial to consider all this while creating rehabilitation exercises for them. Some recommendations stated by *Fischer et al.* [108] are to reduce interface complexity, improve executive function, use large text, and use the right lighting.

6. Conclusions

Robotic rehabilitation in combination with VR enables more intense and motivating exercises, but there is still a lack of evidence on how the interaction with the VE while using a robot and its visualization can influence motor recovery and motivation. In this study, we develop a digital twin of an upper-limb rehabilitation exoskeleton robot in a VE, portraying the user's reality when in a robotic rehabilitation session. To achieve this goal, our work was divided into two main parts: the integration of a hand module into the rehabilitation exoskeleton and the development and integration of the DT in a VE.

Our results suggest that the integration of the hand module allowed the user to perform grasping movements. Since this is one of the essential movements practiced in ADLs, it will allow the user to perform more complete rehabilitation exercises. Regarding the DT, each joint was connected and linked to generate a kinematic system similar to that of the real robot. The DT was connected to the exoskeleton, retrieving its data, and mimicking its movements. Using VR instead of a computer screen to visualize and interact with the DT created conditions to develop more immersive and motivating rehabilitation exercises. Through the evaluation of kinematic accuracy, it was found that the position deviation between the real robot and the DT was low and therefore suggests that for low values in the centimeter range, the user will not be affected in terms of immersion. Furthermore, we were able to perform simple tasks in the virtual environment with the DT, allowing it to interact with the VE and enabling the creation of relevant rehabilitation exercises on this basis.

The concept of digital twins is relatively new and therefore there is little literature on their applications, especially in the field of upper limb rehabilitation. While our research is a starting point to better understand how this technology can be applied to this field, there are still some areas that need improvement. The data from the integrated hand module should be linked to the digital twin to allow the user to see each movement reflected in the virtual environment, as well as adjust the joints of the digital twin to further reduce the recorded position offset. Further studies and user surveys should also be conducted to access the benefits of our work and to better adjust it to their needs.

Nonetheless, this study opens innovative investigation possibilities. Firstly, since the DT and VE are fully customizable, it allows us to study how the user reacts to different characteristics and how this influences motor recovery. Mainly, we can assess what characteristics influence positively the user's motor recovery and create more personalized exercises. Additionally, we hope that our work will raise awareness of the applicability of DT in the rehabilitation field. Our study may then contribute to the study and understanding of better rehabilitation processes after stroke, enhancing post-stroke people's recovery and thus improving their future quality of life.

References

[1] R. Rätz, F. Conti, R. M. Müri, and L. Marchal-Crespo, "A Novel Clinical-Driven Design for Robotic Hand Rehabilitation: Combining Sensory Training, Effortless Setup, and Large Range of Motion in a Palmar Device," *Front Neurorobot*, vol. 15, Dec. 2021, doi: 10.3389/fnbot.2021.748196.

[2] V. L. Feigin *et al.*, "World Stroke Organization (WSO): Global Stroke Fact Sheet 2022," *International Journal of Stroke*, vol. 17, no. 1, pp. 18–29, Jan. 2022, doi: 10.1177/17474930211065917.

[3] S. M. Lai, S. Studenski, P. W. Duncan, and S. Perera, "Persisting consequences of stroke measured by the Stroke Impact Scale," *Stroke*, vol. 33, no. 7, pp. 1840–1844, 2002, doi: 10.1161/01.STR.0000019289.15440.F2.

[4] V. M. Parker, D. T. Wade, and R. L. Hewer, "Loss of arm function after stroke: measurement, frequency, and recovery," *Int Rehabil Med*, vol. 8, no. 2, pp. 69–73, 1986, doi: 10.3109/03790798609166178.

[5] L. Y. Liu, Y. Li, and A. Lamontagne, "The effects of error-augmentation versus error-reduction paradigms in robotic therapy to enhance upper extremity performance and recovery post-stroke: a systematic review," *J Neuroeng Rehabil*, vol. 15, no. 1, Jul. 2018, doi: 10.1186/S12984-018-0408-5.

[6] J. Bo Nielsen, M. Willerslev-Olsen, L. Christiansen, J. Lundbye-Jensen, and J. Lorentzen, "Science-based neurorehabilitation: recommendations for neurorehabilitation from basic science," *J Mot Behav*, vol. 47, no. 1, pp. 7–17, Jan. 2015, doi: 10.1080/00222895.2014.931273.

[7] S. R. Zeiler and J. W. Krakauer, "The interaction between training and plasticity in the post-stroke brain," *Curr Opin Neurol*, vol. 26, no. 6, p. 609, Dec. 2013, doi: 10.1097/WCO.0000000000000025.

[8] R. Gassert and V. Dietz, "Rehabilitation robots for the treatment of sensorimotor deficits: A neurophysiological perspective," *Journal of NeuroEngineering and Rehabilitation*, vol. 15, no. 1. BioMed Central Ltd., Jun. 05, 2018. doi: 10.1186/s12984-018-0383-x.

[9] C. E. Lang *et al.*, "Observation of Amounts of Movement Practice Provided During Stroke Rehabilitation," *Arch Phys Med Rehabil*, vol. 90, no. 10, pp. 1692–1698, Oct. 2009, doi: 10.1016/j.apmr.2009.04.005.

[10] M. da Silva Cameiro, S. Bermúdez I Badia, E. Duarte, and P. F. M. J. Verschure, "Virtual reality based rehabilitation speeds up functional recovery of the upper extremities after stroke: A randomized controlled pilot study in the acute phase of stroke using the Rehabilitation Gaming System," *Restor Neurol Neurosci*, vol. 29, no. 5, pp. 287–298, 2011, doi: 10.3233/RNN-2011-0599.

[11] M. F. Levin Pt, P. L. Weiss Ot, and E. A. Keshner Pt, "Emergence of virtual reality as a tool for upper limb rehabilitation: Incorporation of motor control and motor learning Principles," *Phys Ther*, vol. 95, no. 3, pp. 415–425, Mar. 2015, doi: 10.2522/ptj.20130579.

[12] D. Charles, D. Holmes, T. Charles, and S. McDonough, "Virtual Reality Design for Stroke Rehabilitation," *Adv Exp Med Biol*, vol. 1235, pp. 53–87, 2020, doi: 10.1007/978-3-030-37639-0_4/TABLES/10.

[13] M. K. Holden, "Virtual environments for motor rehabilitation: review," *Cyberpsychol Behav*, vol. 8, no. 3, pp. 187–211, Jun. 2005, doi: 10.1089/CPB.2005.8.187.

[14] H. J. Sung *et al.*, "Cortical reorganization and associated functional motor recovery after virtual reality in patients with chronic stroke: an experimenter-blind preliminary study," *Arch Phys Med Rehabil*, vol. 86, no. 11, pp. 2218–2223, Nov. 2005, doi: 10.1016/J.APMR.2005.04.015.

[15] Boff, K. R., Kaufman, L., & Thomas, J. P. (Eds.). (1986). Handbook of perception and human performance, Vol. 2. Cognitive processes and performance. John Wiley & Sons.

[16] A. Mirelman, P. Bonato, and J. E. Deutsch, "Effects of training with a robot-virtual reality system compared with a robot alone on the gait of individuals after stroke," *Stroke*, vol. 40, no. 1, pp. 169–174, Jan. 2009, doi: 10.1161/STROKEAHA.108.516328.

[17] M. S. Martin Usoh and A. Steed, "Taking Steps: The Influence of a Walking Technique on Presence in Virtual Reality," *ACM Transactions on Computer-Human Interaction (TOCHI)*, vol. 2, no. 3, pp. 201–219, 1995, doi: 10.1145/210079.210084.

[18] N. Wenk *et al.*, "Reaching in Several Realities: Motor and Cognitive Benefits of Different Visualization Technologies," in *2019 IEEE 16th International Conference on Rehabilitation Robotics (ICORR)*, 2019, pp. 1037–1042. doi: 10.1109/ICORR.2019.8779366.

[19] J. W. Burke, M. D. J. McNeill, D. K. Charles, P. J. Morrow, J. H. Crosbie, and S. M. McDonough, "Optimising engagement for stroke rehabilitation using serious games," *Visual Computer*, vol. 25, no. 12, pp. 1085–1099, 2009, doi: 10.1007/s00371-009-0387-4.

[20] S. H. Lee, H. Y. Jung, S. J. Yun, B. M. Oh, and H. G. Seo, "Upper Extremity Rehabilitation Using Fully Immersive Virtual Reality Games With a Head Mount Display: A Feasibility Study," *PM and R*, vol. 12, no. 3, pp. 257–262, Mar. 2020, doi: 10.1002/pmrj.12206.

[21] L. M. Weber, D. M. Nilsen, G. Gillen, J. Yoon, and J. Stein, "Immersive virtual reality mirror therapy for upper limb recovery following stroke: A pilot study," *Am J Phys Med Rehabil*, vol. 98, no. 9, p. 783, Sep. 2019, doi: 10.1097/PHM.0000000000001190.

[22] S. Ojaghihaghighi, S. S. Vahdati, A. Mikaeilpour, and A. Ramouz, "Comparison of neurological clinical manifestation in patients with hemorrhagic and ischemic stroke," *World J Emerg Med*, vol. 8, no. 1, p. 34, 2017, doi: 10.5847/WJEM.J.1920-8642.2017.01.006.

[23] "Stroke - What Is a Stroke? | NHLBI, NIH." https://www.nhlbi.nih.gov/health/stroke (accessed Dec. 03, 2022).

[24] "What is Atherosclerosis? | American Heart Association." https://www.heart.org/en/health-topics/cholesterol/about-cholesterol/atherosclerosis (accessed Jan. 11, 2023).

[25] A. HP *et al.*, "Classification of subtype of acute ischemic stroke. Definitions for use in a multicenter clinical trial. TOAST. Trial of Org 10172 in Acute Stroke Treatment," *Stroke*, vol. 24, no. 1, pp. 35–41, 1993, doi: 10.1161/01.STR.24.1.35.

[26] J. W. Chung *et al.*, "Trial of ORG 10172 in Acute Stroke Treatment (TOAST) Classification and Vascular Territory of Ischemic Stroke Lesions Diagnosed by Diffusion-Weighted Imaging," *J Am Heart Assoc*, vol. 3, no. 4, Aug. 2014, doi: 10.1161/JAHA.114.001119.

[27] J. Bogousslavsky, G. van Melle, and F. Regli, "The Lausanne Stroke Registry: analysis of 1,000 consecutive patients with first stroke," *Stroke*, vol. 19, no. 9, pp. 1083–1092, 1988, doi: 10.1161/01.STR.19.9.1083.

[28] K. Rajdev, S. Lahan, K. Klein, C. A. Piquette, and M. Thi, "Acute Ischemic and Hemorrhagic Stroke in COVID-19: Mounting Evidence," *Cureus*, vol. 12, no. 8, Aug. 2020, doi: 10.7759/CUREUS.10157.

[29] K. Hardie, G. J. Hankey, K. Jamrozik, R. J. Broadhurst, and C. Anderson, "Ten-year survival after first-ever stroke in the perth community stroke study," *Stroke*, vol. 34, no. 8, pp. 1842–1846, Aug. 2003, doi: 10.1161/01.STR.0000082382.42061.EE.

[30] C. S. Anderson, K. N. Carter, W. J. Brownlee, M. L. Hackett, J. B. Broad, and R. Bonita, "Very long-term outcome after stroke in Auckland, New Zealand," *Stroke*, vol. 35, no. 8, pp. 1920–1924,

Aug. 2004, doi: 10.1161/01.STR.0000133130.20322.9F.
[31] G. Boysen, J. L. Marott, M. Grønbæk, H. Hassanpour, and T. Truelsen, "Long-term survival after stroke: 30 Years of follow-up in a cohort, the Copenhagen City Heart Study," *Neuroepidemiology*, vol. 33, no. 3, pp. 254–260, Oct. 2009, doi: 10.1159/000229780.
[32] M. A. Dimyan and L. G. Cohen, "Neuroplasticity in the context of motor rehabilitation after stroke," *Nat Rev Neurol*, vol. 7, no. 2, pp. 76–85, Feb. 2011, doi: 10.1038/NRNEUROL.2010.200.
[33] T. E. Twitchell, "THE RESTORATION OF MOTOR FUNCTION FOLLOWING HEMIPLEGIA IN MAN," *Brain*, vol. 74, no. 4, pp. 443–480, Dec. 1951, doi: 10.1093/BRAIN/74.4.443.
[34] G. Kwakkel, B. Kollen, and E. Lindeman, "Understanding the pattern of functional recovery after stroke: Facts and theories," *Restor Neurol Neurosci*, vol. 22, pp. 281–299, 2004.
[35] L. Brewer, F. Horgan, A. Hickey, and D. Williams, "Stroke rehabilitation: Recent advances and future therapies," *QJM*, vol. 106, Nov. 2012, doi: 10.1093/qjmed/hcs174.
[36] C. Gerloff *et al.*, "Multimodal imaging of brain reorganization in motor areas of the contralesional hemisphere of well recovered patients after capsular stroke," *Brain*, vol. 129, no. 3, pp. 791–808, Mar. 2006, doi: 10.1093/BRAIN/AWH713.
[37] R. J. Nudo, "Recovery after brain injury: Mechanisms and principles," *Front Hum Neurosci*, vol. 7, no. DEC, p. 887, Dec. 2013, doi: 10.3389/FNHUM.2013.00887/BIBTEX.
[38] L. C. Rodrigues, N. C. Farias, R. P. Gomes, and S. M. Michaelsen, "Feasibility and effectiveness of adding object-related bilateral symmetrical training to mirror therapy in chronic stroke: A randomized controlled pilot study," *Physiother Theory Pract*, vol. 32, no. 2, pp. 83–91, Feb. 2016, doi: 10.3109/09593985.2015.1091872.
[39] M. E. Greenberg, B. Xu, B. Lu, and B. L. Hempstead, "New insights in the biology of BDNF synthesis and release: implications in CNS function," *J Neurosci*, vol. 29, no. 41, pp. 12764–12767, Oct. 2009, doi: 10.1523/JNEUROSCI.3566-09.2009.
[40] W. R. Schabitz *et al.*, "Intravenous brain-derived neurotrophic factor reduces infarct size and counterregulates Bax and Bcl-2 expression after temporary focal cerebral ischemia," *Stroke*, vol. 31, no. 9, pp. 2212–2217, 2000, doi: 10.1161/01.STR.31.9.2212.
[41] J. Biernaskie, G. Chernenko, and D. Corbett, "Efficacy of Rehabilitative Experience Declines with Time after Focal Ischemic Brain Injury," *Journal of Neuroscience*, vol. 24, no. 5, pp. 1245–1254, Feb. 2004, doi: 10.1523/JNEUROSCI.3834-03.2004.
[42] H. S. Jorgensen, H. Nakayama, H. O. Raaschou, and T. S. Olsen, "Stroke: Neurologic and Functional Recovery The Copenhagen Stroke Study," *Phys Med Rehabil Clin N Am*, vol. 10, no. 4, pp. 887–906, Nov. 1999, doi: 10.1016/S1047-9651(18)30169-4.
[43] N. S. Ward, M. M. Brown, A. J. Thompson, and R. S. J. Frackowiak, "Neural correlates of motor recovery after stroke: a longitudinal fMRI study," *Brain*, vol. 126, no. 11, pp. 2476–2496, Nov. 2003, doi: 10.1093/BRAIN/AWG245.
[44] P. Langhorne, J. Bernhardt, and G. Kwakkel, "Stroke rehabilitation," *The Lancet*, vol. 377, no. 9778, pp. 1693–1702, May 2011, doi: 10.1016/S0140-6736(11)60325-5.
[45] P. Raghavan, M. Santello, A. M. Gordon, and J. W. Krakauer, "Compensatory motor control after stroke: an alternative joint strategy for object-dependent shaping of hand posture," *J Neurophysiol*, vol. 103, no. 6, pp. 3034–3043, Jun. 2010, doi: 10.1152/JN.00936.2009.
[46] J. W. Krakauer, S. T. Carmichael, D. Corbett, and G. F. Wittenberg, "Getting neurorehabilitation right: what can be learned from animal models?," *Neurorehabil Neural Repair*, vol. 26, no. 8, pp. 923–931, Oct. 2012, doi: 10.1177/1545968312440745.

[47] A. R. Fugl Meyer, L. Jaasko, and I. Leyman, “The post stroke hemiplegic patient. I. A method for evaluation of physical performance,” *Scand J Rehabil Med*, vol. 7, no. 1, pp. 13–31, 1975.

[48] D. J. Gladstone, C. J. Danells, and S. E. Black, “The fugl-meyer assessment of motor recovery after stroke: a critical review of its measurement properties,” *Neurorehabil Neural Repair*, vol. 16, no. 3, pp. 232–240, 2002, doi: 10.1177/154596802401105171.

[49] S. H. Lee *et al.*, “Comparisons between end-effector and exoskeleton rehabilitation robots regarding upper extremity function among chronic stroke patients with moderate-to-severe upper limb impairment,” *Sci Rep*, vol. 10, no. 1, Dec. 2020, doi: 10.1038/s41598-020-58630-2.

[50] H. F. Mao, I. P. Hsueh, P. F. Tang, C. F. Sheu, and C. L. Hsieh, “Analysis and Comparison of the Psychometric Properties of Three Balance Measures for Stroke Patients,” *Stroke*, vol. 33, no. 4, pp. 1022–1027, Apr. 2002, doi: 10.1161/01.STR.0000012516.63191.C5.

[51] S. L. Wolf, P. A. Catlin, M. Ellis, A. Link Archer, B. Morgan, and A. Piacentino, “Assessing Wolf Motor Function Test as Outcome Measure for Research in Patients After Stroke,” 2001.

[52] M. Ferraro *et al.*, “Assessing the motor status score: a scale for the evaluation of upper limb motor outcomes in patients after stroke,” *Neurorehabil Neural Repair*, vol. 16, no. 3, pp. 283–289, 2002, doi: 10.1177/154596830201600306.

[53] I. Carpinella, D. Cattaneo, and M. Ferrarin, “Quantitative assessment of upper limb motor function in Multiple Sclerosis using an instrumented Action Research Arm Test,” *J Neuroeng Rehabil*, vol. 11, no. 1, pp. 1–16, Apr. 2014, doi: 10.1186/1743-0003-11-67/FIGURES/9.

[54] J. Desrosiers, G. Bravo, R. Hébert, É. Dutil, and L. Mercier, “Validation of the Box and Block Test as a measure of dexterity of elderly people: Reliability, validity, and norms studies,” *Arch Phys Med Rehabil*, vol. 75, no. 7, pp. 751–755, Jul. 1994, doi: 10.1016/0003-9993(94)90130-9.

[55] J. Hidler, D. Nichols, M. Pelliccio, and K. Brady, “Advances in the understanding and treatment of stroke impairment using robotic devices,” *Top Stroke Rehabil*, vol. 12, no. 2, pp. 22–35, Mar. 2005, doi: 10.1310/RYT5-62N4-CTVX-8JTE.

[56] J. Mehrholz, M. Pohl, T. Platz, J. Kugler, and B. Elsner, “Electromechanical and robot-assisted arm training for improving activities of daily living, arm function, and arm muscle strength after stroke,” *Cochrane Database Syst Rev*, vol. 9, no. 9, Sep. 2018, doi: 10.1002/14651858.CD006876.PUB5.

[57] M. L. Aisen, H. I. Krebs, N. Hogan, F. McDowell, and B. T. Volpe, “The effect of robot-assisted therapy and rehabilitative training on motor recovery following stroke,” *Arch Neurol*, vol. 54, no. 4, pp. 443–446, 1997, doi: 10.1001/ARCHNEUR.1997.00550160075019.

[58] P. Maciejasz, J. Eschweiler, K. Gerlach-Hahn, A. Jansen-Troy, and S. Leonhardt, “JNER JOURNAL OF NEUROENGINEERING AND REHABILITATION REVIEW Open Access A survey on robotic devices for upper limb rehabilitation,” *J Neuroeng Rehabil*, vol. 11, p. 3, 2014.

[59] H. I. Krebs, N. Hogan, M. L. Aisen, and B. T. Volpe, “Robot-Aided Neurorehabilitation,” 1998.

[60] A. S. Gorgey, “Robotic exoskeletons: The current pros and cons,” *World J Orthop*, vol. 9, no. 9, pp. 112–119, Sep. 2018, doi: 10.5312/WJO.V9.I9.112.

[61] H. S. Lo and S. Q. Xie, “Exoskeleton robots for upper-limb rehabilitation: state of the art and future prospects,” *Med Eng Phys*, vol. 34, no. 3, pp. 261–268, Apr. 2012, doi: 10.1016/J.MEDENGPHY.2011.10.004.

[62] H. Kazerooni, “The berkeley lower extremity exoskeleton,” *Springer Tracts in Advanced Robotics*, vol. 25, pp. 9–15, 2006, doi: 10.1007/978-3-540-33453-8_2/COVER.

[63] H. Lee, W. Kim, J. Han, and C. Han, “The technical trend of the exoskeleton robot system for human power assistance,” *International Journal of Precision Engineering and Manufacturing*, vol. 13, no.

8, pp. 1491–1497, 2012, doi: 10.1007/S12541-012-0197-X.

[64] N. Rehmat, J. Zuo, W. Meng, Q. Liu, S. Q. Xie, and H. Liang, "Upper limb rehabilitation using robotic exoskeleton systems: a systematic review," *Int J Intell Robot Appl*, vol. 2, no. 3, pp. 283–295, Sep. 2018, doi: 10.1007/s41315-018-0064-8.

[65] "Armeo®Spring - Hocoma." https://www.hocoma.com/solutions/armeo-spring/ (accessed Nov. 09, 2022).

[66] J. C. Perry, J. Rosen, and S. Burns, "Upper-limb powered exoskeleton design," in *IEEE/ASME Transactions on Mechatronics*, Aug. 2007, vol. 12, no. 4, pp. 408–417. doi: 10.1109/TMECH.2007.901934.

[67] T. Rahman *et al.*, "Passive exoskeletons for assisting limb movement," *J Rehabil Res Dev*, vol. 43, no. 5, pp. 583–589, Sep. 2006, doi: 10.1682/JRRD.2005.04.0070.

[68] S. Balasubramanian *et al.*, "Rupert: An exoskeleton robot for assisting rehabilitation of arm functions," *2008 Virtual Rehabilitation, IWVR*, pp. 163–167, 2008, doi: 10.1109/ICVR.2008.4625154.

[69] S. Balasubramanian, J. Klein, and E. Burdet, "Robot-assisted rehabilitation of hand function," *Curr Opin Neurol*, vol. 23, no. 6, pp. 661–670, Dec. 2010, doi: 10.1097/WCO.0B013E32833E99A4.

[70] J. T. Bell and H. S. Fogler, "The application of virtual reality to (chemical engineering) education," *Proceedings - Virtual Reality Annual International Symposium*, pp. 217–218, 2004, doi: 10.1109/VR.2004.1310077.

[71] "DSTS: First immersive virtual training system fielded | Article | The United States Army." https://www.army.mil/article/84728/DSTS__First_immersive_virtual_training_system_fielded (accessed Nov. 18, 2022).

[72] A. O. Dourado and C. A. Martin, "New concept of dynamic flight simulator, Part I," *Aerosp Sci Technol*, vol. 30, no. 1, pp. 79–82, Oct. 2013, doi: 10.1016/J.AST.2013.07.005.

[73] C. Moro, Z. Štromberga, A. Raikos, and A. Stirling, "The effectiveness of virtual and augmented reality in health sciences and medical anatomy," *Anat Sci Educ*, vol. 10, no. 6, pp. 549–559, Nov. 2017, doi: 10.1002/ASE.1696.

[74] G. M. Lemole, P. P. Banerjee, C. Luciano, S. Neckrysh, and F. T. Charbel, "Virtual reality in neurosurgical education: Part-task ventriculostomy simulation with dynamic visual and haptic feedback," *Neurosurgery*, vol. 61, no. 1, pp. 142–148, Jul. 2007, doi: 10.1227/01.neu.0000279734.22931.21.

[75] M. Gerardi, J. Cukor, J. Difede, A. Rizzo, and B. O. Rothbaum, "Virtual reality exposure therapy for post-traumatic stress disorder and other anxiety disorders.," *Curr Psychiatry Rep*, vol. 12, no. 4, pp. 298–305, Jun. 2010, doi: 10.1007/S11920-010-0128-4/FIGURES/4.

[76] F. Clay, D. Howett, J. FitzGerald, P. Fletcher, D. Chan, and A. Price, "Use of Immersive Virtual Reality in the Assessment and Treatment of Alzheimer's Disease: A Systematic Review," *Journal of Alzheimer's Disease*, vol. 75, no. 1, p. 23, Apr. 2020, doi: 10.3233/JAD-191218.

[77] D. D. Georgiev, I. Georgieva, Z. Gong, V. Nanjappan, and G. v. Georgiev, "Virtual Reality for Neurorehabilitation and Cognitive Enhancement," *Brain Sci*, vol. 11, no. 2, pp. 1–20, Feb. 2021, doi: 10.3390/BRAINSCI11020221.

[78] S. A. E. Nooij, P. Pretto, D. Oberfeld, H. Hecht, and H. H. Bülthoff, "Vection is the main contributor to motion sickness induced by visual yaw rotation: Implications for conflict and eye movement theories," *PLoS One*, vol. 12, no. 4, p. e0175305, Apr. 2017, doi: 10.1371/JOURNAL.PONE.0175305.

[79] X. Li, C. Zhu, C. Xu, J. Zhu, Y. Li, and S. Wu, "VR motion sickness recognition by using EEG rhythm energy ratio based on wavelet packet transform," *Comput Methods Programs Biomed*, vol. 188, May 2020, doi: 10.1016/J.CMPB.2019.105266.

[80] J. O. Brooks *et al.*, "Simulator sickness during driving simulation studies," *Accid Anal Prev*, vol. 42, no. 3, pp. 788–796, May 2010, doi: 10.1016/J.AAP.2009.04.013.

[81] C. J. Bohil, B. Alicea, and F. A. Biocca, "Virtual reality in neuroscience research and therapy," *Nat Rev Neurosci*, vol. 12, no. 12, Dec. 2011, doi: 10.1038/NRN3122.

[82] O. Blanke, "Multisensory brain mechanisms of bodily self-consciousness," *Nature Reviews Neuroscience 2012 13:8*, vol. 13, no. 8, pp. 556–571, Jul. 2012, doi: 10.1038/nrn3292.

[83] N. Wenk, J. Penalver-Andres, K. A. Buetler, T. Nef, R. M. Müri, and L. Marchal-Crespo, "Effect of immersive visualization technologies on cognitive load, motivation, usability, and embodiment," *Virtual Reality 2021*, vol. 1, pp. 1–25, Aug. 2021, doi: 10.1007/S10055-021-00565-8.

[84] W. S. Kim *et al.*, "Clinical Application of Virtual Reality for Upper Limb Motor Rehabilitation in Stroke: Review of Technologies and Clinical Evidence," *J Clin Med*, vol. 9, no. 10, pp. 1–20, Oct. 2020, doi: 10.3390/JCM9103369.

[85] H. J. Sung *et al.*, "Cortical reorganization and associated functional motor recovery after virtual reality in patients with chronic stroke: an experimenter-blind preliminary study," *Arch Phys Med Rehabil*, vol. 86, no. 11, pp. 2218–2223, Nov. 2005, doi: 10.1016/J.APMR.2005.04.015.

[86] N. Wenk, M. v Jordi, K. A. Buetler, and L. Marchal-Crespo, "Hiding Assistive Robots During Training in Immersive VR Does Not Affect Users' Motivation, Presence, Embodiment, Performance, Nor Visual Attention," *IEEE TRANSACTIONS ON NEURAL SYSTEMS AND REHABILITATION ENGINEERING*, vol. 30, p. 2022, doi: 10.1109/TNSRE.2022.3147260.

[87] "Varjo XR-3 - The industry's highest resolution XR headset | Varjo." https://varjo.com/products/xr-3/ (accessed Nov. 19, 2022).

[88] A. Manuli *et al.*, "Can robotic gait rehabilitation plus Virtual Reality affect cognitive and behavioural outcomes in patients with chronic stroke? A randomized controlled trial involving three different protocols," *Journal of Stroke and Cerebrovascular Diseases*, vol. 29, no. 8, Aug. 2020, doi: 10.1016/j.jstrokecerebrovasdis.2020.104994.

[89] S. H. Lee, H. Y. Jung, S. J. Yun, B. M. Oh, and H. G. Seo, "Upper Extremity Rehabilitation Using Fully Immersive Virtual Reality Games With a Head Mount Display: A Feasibility Study," *PM and R*, vol. 12, no. 3, pp. 257–262, Mar. 2020, doi: 10.1002/pmrj.12206.

[90] C. Christou, D. Michael-Grigoriou, D. Sokratous, and M. Tsiakoulia, "A virtual reality loop and wire game for stroke rehabilitation," 2018.

[91] L. M. Weber, D. M. Nilsen, G. Gillen, J. Yoon, and J. Stein, "Immersive virtual reality mirror therapy for upper limb recovery following stroke: A pilot study," *Am J Phys Med Rehabil*, vol. 98, no. 9, p. 783, Sep. 2019, doi: 10.1097/PHM.0000000000001190.

[92] S. C. Gobron *et al.*, "Serious games for rehabilitation using Head-Mounted display and haptic devices," *Lecture Notes in Computer Science (including subseries Lecture Notes in Artificial Intelligence and Lecture Notes in Bioinformatics)*, vol. 9254, pp. 199–219, 2015, doi: 10.1007/978-3-319-22888-4_15.

[93] J. W. Burke, M. D. J. McNeill, D. K. Charles, P. J. Morrow, J. H. Crosbie, and S. M. McDonough, "Optimising engagement for stroke rehabilitation using serious games," *Visual Computer*, vol. 25, no. 12, pp. 1085–1099, 2009, doi: 10.1007/s00371-009-0387-4.

[94] M. Mihelj, D. Novak, M. Milavec, J. Ziherl, A. Olenšek, and M. Munih, "Virtual Rehabilitation

Environment Using Principles of Intrinsic Motivation and Game Design," *Presence: Teleoperators and Virtual Environments*, vol. 21, no. 1, pp. 1–15, Feb. 2012, doi: 10.1162/PRES_a_00078.

[95] J. P. Gee, "What video games have to teach us about learning and literacy," *Comput. Entertain.*, vol. 1, p. 20, 2003.

[96] M. Mihelj, D. Novak, M. Milavec, J. Ziherl, A. Olenšek, and M. Munih, "Virtual Rehabilitation Environment Using Principles of Intrinsic Motivation and Game Design," *Presence: Teleoperators and Virtual Environments*, vol. 21, no. 1, pp. 1–15, Feb. 2012, doi: 10.1162/PRES_a_00078.

[97] G. M. C. Martínez and L. A. Z. Avilés, "Design Methodology for Rehabilitation Robots: Application in an Exoskeleton for Upper Limb Rehabilitation," *Applied Sciences 2020, Vol. 10, Page 5459*, vol. 10, no. 16, p. 5459, Aug. 2020, doi: 10.3390/APP10165459.

[98] Grieves, Michael. (2002). SME Management Forum Completing the Cycle: Using PLM Information in the Sales and Service Functions.

[99] S. F. R. Alves, A. Uribe-Quevedo, D. Chen, J. Morris, and S. Radmard, "Developing a VR Simulator for Robotics Navigation and Human Robot Interactions employing Digital Twins," *Proceedings - 2022 IEEE Conference on Virtual Reality and 3D User Interfaces Abstracts and Workshops, VRW 2022*, pp. 121–125, 2022, doi: 10.1109/VRW55335.2022.00036.

[100] F. Tao, H. Zhang, A. Liu, and A. Y. C. Nee, "Digital Twin in Industry: State-of-the-Art," *IEEE Trans Industr Inform*, vol. 15, no. 4, pp. 2405–2415, Apr. 2019, doi: 10.1109/TII.2018.2873186.

[101] E. J. Tuegel, A. R. Ingraffea, T. G. Eason, and S. M. Spottswood, "Reengineering aircraft structural life prediction using a digital twin," *International Journal of Aerospace Engineering*, 2011, doi: 10.1155/2011/154798.

[102] M. Hummel and K. van Kooten, "Leveraging NVIDIA Omniverse for In Situ Visualization," *Lecture Notes in Computer Science (including subseries Lecture Notes in Artificial Intelligence and Lecture Notes in Bioinformatics)*, vol. 11887 LNCS, pp. 634–642, 2019, doi: 10.1007/978-3-030-34356-9_48/COVER.

[103] C. Pizzolato *et al.*, "Neuromusculoskeletal Modeling-Based Prostheses for Recovery After Spinal Cord Injury," *Front Neurorobot*, vol. 13, 2019, doi: 10.3389/FNBOT.2019.00097.

[104] B. Baillargeon, N. Rebelo, D. D. Fox, R. L. Taylor, and E. Kuhl, "The living heart project: A robust and integrative simulator for human heart function," *European Journal of Mechanics, A/Solids*, vol. 48, no. 1, pp. 38–47, 2014, doi: 10.1016/j.euromechsol.2014.04.001.

[105] A. Topini, W. Sansom, N. Secciani, L. Bartalucci, A. Ridolfi, and B. Allotta, "Variable Admittance Control of a Hand Exoskeleton for Virtual Reality-Based Rehabilitation Tasks," *Front Neurorobot*, vol. 15, p. 789743, Jan. 2021, doi: 10.3389/FNBOT.2021.789743.

[106] I. Voigt, H. Inojosa, A. Dillenseger, R. Haase, K. Akgün, and T. Ziemssen, "Digital Twins for Multiple Sclerosis," *Front Immunol*, vol. 12, p. 1556, May 2021, doi: 10.3389/FIMMU.2021.669811/BIBTEX.

[107] A. Holzinger, G. Searle, and A. N. Witzer, "On some aspects of improving mobile applications for the elderly," *Lecture Notes in Computer Science (including subseries Lecture Notes in Artificial Intelligence and Lecture Notes in Bioinformatics)*, vol. 4554 LNCS, no. PART 1, pp. 923–932, 2007, doi: 10.1007/978-3-540-73279-2_103/COVER.

[108] S. H. Fischer, D. David, B. H. Crotty, M. Dierks, and C. Safran, "Acceptance and use of health information technology by community-dwelling elders," *Int J Med Inform*, vol. 83, no. 9, pp. 624–635, Sep. 2014, doi: 10.1016/J.IJMEDINF.2014.06.005.

[109] M. Guidali, A. Duschau-Wicke, S. Broggi, V. Klamroth-Marganska, T. Nef, and R. Riener, "A

robotic system to train activities of daily living in a virtual environment," *Med Biol Eng Comput*, vol. 49, no. 10, pp. 1213–1223, Oct. 2011, doi: 10.1007/S11517-011-0809-0.

[110] T. M. Shank, J. Wee, J. Ty, and T. Rahman, "Quantitative measures with WREX usage," *IEEE Int Conf Rehabil Robot*, vol. 2017, pp. 1375–1380, Aug. 2017, doi: 10.1109/ICORR.2017.8009440.

[111] M. Dębska, J. Polechoński, A. Mynarski, and P. Polechoński, "Enjoyment and Intensity of Physical Activity in Immersive Virtual Reality Performed on Innovative Training Devices in Compliance with Recommendations for Health," *International Journal of Environmental Research and Public Health 2019, Vol. 16, Page 3673*, vol. 16, no. 19, p. 3673, Sep. 2019, doi: 10.3390/IJERPH16193673.